Applied Geochemistry 63 (2015) 456–471

Contents lists available at ScienceDirect

Applied Geochemistry

journal homepage: www.elsevier.com/locate/apgeochem

Hydrochemical variations of a tropical mountain river system in a rain shadow region of the southern Western Ghats, Kerala, India

Jobin Thomas [a, *], Sabu Joseph [a], K.P. Thrivikramji [b]

[a] Department of Environmental Sciences, University of Kerala, Thiruvananthapuram 695 581, Kerala, India
[b] Center for Environment and Development, Thiruvananthapuram 695 013, Kerala, India

ARTICLE INFO

Article history:
Received 7 April 2014
Received in revised form
28 March 2015
Accepted 30 March 2015
Available online 9 April 2015

Keywords:
Hydrochemistry
Rain shadow rivers
Weathering
Downstream hydrochemical trend
Southern Western Ghats

ABSTRACT

River water chemistry of Pambar River Basin (PRB), draining a rain shadow region of the southern Western Ghats, India, with granite gneiss and hornblende-biotite-gneiss lithology, was monitored for three sampling seasons, such as monsoon (MON), post-monsoon (POM) and pre-monsoon (PRM) to ascertain the spatio-temporal trends in hydrochemistry. In PRB, upstream and downstream areas have differing climate (i.e., tropical-wet–dry/humid upstream, while semi-arid downstream) and land use (plantations and farmland dominate the upstream, while pristine forest environment covers the downstream). The hydrochemical attributes, except pH and K^+, exhibit distinct temporal variation mainly due to monsoon-driven climatic seasonality. Relative abundance of cations between upstream and downstream samples of PRB shows noticeable differences, in that the upstream samples follow the order of abundance: $Ca^{2+} > Mg^{2+} > Na^+ > K^+$, while the downstream samples are in the order: $Na^+ > Mg^{2+} > Ca^{2+} > K^+$. $Ca^{2+} + Mg^{2+}/Na^+ + K^+$, $Si/Na^+ + K^+$, Cl^-/Na^+ and HCO_3^-/Ca^{2+} ratios suggest multiple sources/processes controlling hydrochemistry, e.g., atmospheric supply, silicate weathering, dissolution of carbonate minerals and soil evaporites as well as anthropogenic inputs (domestic and farm/plantation residues). Even though weathering of silicate and carbonate minerals is the major hydrochemical driver in both upstream and downstream portions of PRB, Gibbs diagram and scatter plot of Mg^{2+}/Na^+ vs. Mg^{2+}/Ca^{2+} imply the importance of evaporation in the downstream hydrochemistry. Piper diagram and partial pressure of CO_2 (pCO_2) values suggest that a groundwater dominated discharge exerts a significant control on the downstream hydrochemistry, irrespective of sampling season. Although spatial variability of rainfall in PRB shows a linear downstream (decreasing) trend, the best-fit model for the dissolved load suggests that the downstream hydrochemical variability in PRB (i.e., an increasing trend) follows a power function ($f(x) = ax^k$). This study suggests that climate has a significant role in the spatio-temporal variability of hydrochemistry in PRB.

1. Introduction

Weathering determinants such as, climate, lithology, tectonics, topography and vegetation are the dominant factors controlling hydrochemical composition of rivers (Gibbs, 1970; Stallard and Edmond, 1981, 1983, 1987; Meybeck, 1987; Drever, 1988; Gaillardet et al., 1999). However, other factors, viz., atmospheric deposition (e.g., aerosols, sea salt spray), contribution from groundwater reservoir as well as anthropogenic inputs via point-(industrial and domestic effluents and wastewater treatment facilities) and diffuse-sources (runoff from urban area and farmlands), also have considerable influences on river water chemistry (Berner and Berner, 1987; Carpenter et al., 1998). But, the relative importance of each hydrochemical driver significantly varies in space and time. Among various hydrochemical determinants, apparent control of climate and lithology on chemical weathering processes and hydrochemistry was explained by various researchers (e.g., Stallard and Edmond, 1983, 1987; Berner and Berner, 1997; Gaillardet et al., 1999). Moreover, surface water chemistry is remarkably sensitive to climate, predominantly to changes in precipitation and temperature (White and Blum, 1995; Dalai et al., 2002; Millot et al., 2002), even in mountainous-headwater-regions (Psenner and Schmidt, 1992; Sommaruga-Wograth et al., 1997). Hence, hydrochemical investigation of river basins provides

* Corresponding author.
E-mail address: jobinenv@gmail.com (J. Thomas).

http://dx.doi.org/10.1016/j.apgeochem.2015.03.018
0883-2927/

adequate information on the rate and pattern of chemical weathering processes and the dissolved elements cycled in the continent–river–ocean system (Hu et al., 1982; Stallard and Edmond, 1983, 1987).

Likewise, spatio-temporal patterns of river water chemistry can also provide unique insights into the hydrologic functioning of catchments (Frohlich et al., 2008) because hydrochemistry of rivers is being regulated by complex interactions among various physical, chemical and biological subsystems in the catchment (Stumm and Morgan, 1996). Spatial variation of river hydrochemistry is principally controlled by tributaries (Meyer et al., 1988), land use (Townsend et al., 1983; Bucker et al., 2010), soil matrix and lithology (Schultz et al., 1993; Stutter et al., 2006; Harmon et al., 2009; Leite et al., 2010) as well as hyporheic zones and groundwater contributions (Boulton et al., 1998, 1999; Banks et al., 2011). On the other hand, temporal variability of river water chemistry is defined predominantly by discharge (Hem, 1948; Smolders et al., 2004; Crosa et al., 2006; Ovalle et al., 2013) and hydrologic pathways (Wheater et al., 1990; Ahearn et al., 2004). In semi-arid and arid rivers, temporal variation of discharge is exceptionally high (due to clearly marked dry and wet seasons) and fluctuations in discharge have enormous effects on hydrochemistry of the rivers (Davies et al., 1994; Allan, 1995).

Hydrochemical composition of the world's largest rivers received greater attention due to their global significance toward water- and sediment-discharge and hydrochemical flux (e.g., Gibbs, 1970; Milliman and Meade, 1983; Gaillardet et al., 1999). Moreover, hydrochemistry of large river systems in the tropics, such as Amazon (Stallard and Edmond, 1981, 1983, 1987; Mortatti and Probst, 2003), Congo (Probst et al., 1992), Gambia (Lesack et al., 1984) and Orinoco (Stallard et al., 1991; Edmond et al., 1996) was also well-documented during the past decades.

After Milliman and Syvitski (1992) and Vegas-Vilarrubia et al. (1994), small mountain river systems in the tropics gained significant attention toward the global dissolved load budget and motivated numerous studies focusing on hydrochemistry and biogeochemistry of these unique systems. Recently, Jennerjahn et al. (2008) recommended mountain rivers of small areal extent as the suitable candidates for biogeochemical process studies because of the shorter response time and easier identification of the effects of individual human activities on water quality and biogeochemistry. In the past decades, several studies (e.g., Lewis et al., 1987; McDowell and Asbury, 1994; Jennerjahn et al., 2004, 2008; Brodie and Mitchell, 2005; Townsend-Small et al., 2008; Harmon et al., 2009; Bucker et al., 2010; Lloret et al., 2011, 2013; Murphy and Stallard, 2012; Moyer et al., 2013) examined the sources and spatio-temporal dynamics of dissolved load, nutrients, sediments and organic matter, and their export to the ocean, which are discussed in the purview of natural processes (e.g., atmospheric input, weathering) and/or anthropogenic activities (e.g., land use changes, pollution, and hydrologic alterations). Many of these contributions also highlighted the vital role of extreme events and climatic seasonality in the elemental flux. Recently, Wohl et al. (2012) suggested the key aspects for integrated research of biogeochemical processes, such as (1) magnitudes and rates of different flow pathways, transport and cycling of carbon and other nutrients; (2) chemical inputs from precipitation, including changes during the year and during an event; (3) the role of dust inputs; and (4) anthropogenic alteration to the systems themselves.

In the Indian context, water chemistry of the Himalayan- as well as the Peninsular-rivers was thoroughly addressed by several researchers (e.g., Subramanian, 1983; Sarin et al., 1992; Galy and France-Lanord, 1999; Das and Krishnaswami, 2006; Jha et al., 2009; Gupta et al., 2011). In addition, spatio-temporal variation in the hydrochemistry /biogeochemistry of west-flowing, smaller river basins (<10,000 km^2; Milliman and Syvitski, 1992) of the Western Ghats, India was also amply discussed (e.g., Prasad and Ramanathan, 2005; Maya et al., 2007; Gurumurthy et al., 2012; Pradhan et al., 2014; Thomas et al., 2014, 2015). Even though a few researchers (e.g., Markich and Brown, 1998; Lecomte et al., 2005) demonstrated the hydrochemical variability of the rivers draining rain shadow regions in other parts of the world, hardly any published data is available on water chemistry of the rivers of the rain shadow regions of the southern Western Ghats, India. Hence, in this paper, we discussed the spatio-temporal variation as well as the processes controlling water chemistry of Pambar, draining a rain shadow region of the southern Western Ghats, Kerala, India.

2. Materials and methods

2.1. Study area

Pambar River Basin (PRB) is a sixth order sub-basin ($A = 288.53$ km^2) of Amaravati River (a major tributary of Cauvery River) and drains between N Lat. 10° 07′ 59″ and 10° 21′ 05″ and E Long. 77° 03′ 24″ and 77° 15′ 32″ (Fig. 1). Pambar is one of the three east-flowing rivers of Kerala, India and elevation of the basin ranges from 2540 to 440 m above mean sea level (msl). The basin is developed mostly on the northern-facing scarps of the Munnar plateau (an extensive planation surface of late Paleocene age; Soman, 2002) and the plateau has a vital role in the drainage network development of PRB (Thomas et al., 2011, 2012).

Due to its NNW–SSE trend and physiography, the Western Ghats acts as a climatic barrier separating tropical humid climate of the western (and windward) slopes and semi-arid climate of the eastern (and leeward) slopes. The drainage network of PRB is developed on a rain shadow segment (of the eastern slopes) of the southern Western Ghats (in Idukki district), Kerala, India. Monsoon is the principal contributor of rainfall in PRB and is spread over two different intervals, viz., the SW monsoon (June–September) and the NE monsoon (October–November). The pre-monsoon (PRM) months (March–May) account for major thunderstorm activity and the winter months (December–February) are characterized by minimum clouding and rainfall. Weather data of PRB for a period of 1992–2008 were gathered from two meteorological stations (viz., Research and Development Division, Talaiyar Tea Ltd. in the upstream portion of PRB and Chinnar Wildlife Sanctuary in the downstream) and examined. Mean annual rainfall (P_{ma}) in the upstream portion of PRB is 1533 mm, while it is only 852 mm in the downstream region. However, several previous studies reported that some locations in the upstream portion of PRB receive 2000–5000 mm of rainfall annually (Jose et al., 1994; Chandrashekara and Sibichan, 2006). In addition, Thomas (2012) observed a linear positive relationship between P_{ma} and altitude in PRB. Contrasting mean monthly rainfall patterns between the upstream and downstream regions of PRB are shown in Fig. 2. Mean annual temperature (T_{ma}) in the upstream part of PRB varies between 20 and 25 °C, while in the downstream segment, T_{ma} is more than 30 °C. Thomas (2012) classified upstream portion of PRB under humid or tropical-wet–dry type, while downstream region as semi-arid using various climate indices and climatic classification schemes.

The drainage network of PRB is formed on the Precambrian Southern Granulite Terrain of the Peninsular India. Major rock types of PRB are hornblende-biotite-gneiss (Hbg) and granite gneiss (Ggn), while pegmatite and dolerite dykes intrude the host rocks (Fig. 3; GSI, 1992). The basement rocks are highly sheared and fractured and have well-developed joint systems. Hbg consists of quartz, plagioclase, K-feldspar as major minerals, while hornblende and biotite are accessories. Hbg shows regular, but alternating

bands rich in quartzo-feldspathic and mafic minerals and individual bands vary both in thickness and mineral composition. On the other hand, Ggn is a medium grained (and pinkish coloured) rock and is foliated due to parallel planar arrangement of flakes of biotite, prisms of hornblende and lenticular as well as flattened quartz veins. In Ggn, mafic layers are thin compared to quartzo-feldspathic layers. Occurrence of laterite as thin layers is also observed around Iravikulam. From the foliation trends in PRB, presence of three major synclinal-axial-traces trending approximately N–S to NE–SW (confined mostly in Hbg) and another major anticlinal-axial-trace of NE–SW trend (appearing in both Hbg and Ggn) is inferred (Fig. 3).

According to SSO (2007), major soil series in PRB are the Anai Mudi series (clayey, mixed, isothermic Typic Kandihumults) and Chinnar series (loamy skeletal, mixed, thermic Typic Haplustolls). Although both the Anai Mudi and Chinnar series are formed on gneissic parent material, the former is mainly distributed (on steep to very steep slopes) at an elevation of 1200 m above msl whereas the latter is formed on gentle slopes at an elevation of 400–900 m above msl. Carbonates (nodules and kankar) and mica flakes are present in the subsurface soil horizons (29–99 cm) of the Chinnar series (SSO, 2007). The Anai Mudi series is very strongly to extremely acidic (pH = 3.9–4.5), while the Chinnar series is neutral to mildly alkaline (pH = 7.0–7.7). Dominant vegetation types of PRB include southern montane wet temperate grassland, southern montane wet temperate forest, southern tropical thorn forest, southern dry mixed deciduous forest and southern moist mixed deciduous forest. Upstream portion of PRB is predominantly covered by Tea (*Camellia sinensis*) and Eucalyptus (e.g., *Eucalyptus grandis*) plantations, whereas the extent of farmlands (e.g., sugarcane and paddy fields, vegetable cultivation) is mainly confined to the central part of the basin.

2.2. Sampling design and analysis

In PRB, 12 river water samples were collected including the main stream and major tributaries (Fig. 1 and Table 1) during three different seasons, viz., monsoon (MON; July 2007), post-monsoon (POM; December 2007) and pre-monsoon (PRM; April 2008), i.e., $12 \times 3 = 36$ samples. At each station, water samples were collected 20–30 cm below water surface in prewashed (with diluted HCl) and labeled HDPE bottles. The sample bottles were pre-rinsed with sample water before acquisition of the final sample. The water samples were filtered through Whatman No: 42 filter papers, and the sediment collected on the filter paper was weighed after drying for determination of total suspended solids (TSS). The filtrate for cation analysis was preserved by acidification with 2 M HNO_3. Each sample was analyzed for various parameters, viz., pH, electrical conductivity (EC), total dissolved solids (TDS), total hardness (TH), total alkalinity (TA), major cations (Ca^{2+}, Mg^{2+}, Na^+ and K^+), major anions (Cl^-, SO_4^{2-} and HCO_3^-) and dissolved silica (Si) following the standard procedures of APHA (Eaton et al., 2005). pH measurements were carried out after calibration with pH 4.0 and 7.0 buffer solutions. Ca^{2+}, Mg^{2+} and TH were estimated by EDTA titration method, while TA and HCO_3^- by acid titration and Cl^- by argentometric method ($AgNO_3$ titration). SO_4^{2-} content in the water samples was measured by spectrophotometry and Na^+ and K^+ were estimated by flame photometry with a precision of ±3%. Si in the river water was measured with UV Spectrophotometer using ammonium molybdate reagent at 410 nm wavelength with a precision of ±2%. All standard solutions were prepared with ultra-pure deionised water. The accuracy of the measurements was checked by measuring freshly prepared standards of known concentrations made from analytical grade reagents and four to five calibration standards were analyzed during each analysis run. However, the samples having concentrations above the highest calibration standard were diluted and reanalyzed. Laboratory blanks were analyzed several times during each analytical run. Each water sample was analyzed in triplicate and the mean value was calculated.

The charge balance (in μeq) between total dissolved cations and total dissolved anions is a reliable measure of the quality of the hydrochemical data. In PRB, river water samples from the mainstream and tributaries show specific charge balance generally better than 10%, which is estimated as Eq. (1):

$$Charge\ Balance = \left[\left(TZ^+ - TZ^-\right) \Big/ TZ^+ + TZ^-\right] \times 100 \quad (1)$$

where TZ^+ and TZ^- are the sum of cations and anions respectively, expressed in μeq.

3. Results and discussion

3.1. Hydrochemical composition and drinking water quality

Table 2 briefly summarizes the 14 hydrochemical variables (as descriptive statistics) of PRB during MON, POM and PRM. Irrespective of the sampling season, pH of river water is nearly neutral and shows only minor temporal variations (Table 2), i.e., 6.75–7.55 (mean = 7.20 ± 0.23) during MON, 6.54–7.70 (mean = 7.11 ± 0.34) during POM and 6.45–7.63 (mean = 7.15 ± 0.31). The degree of mineralization, expressing as EC, shows considerable variability among the seasons, i.e., EC varies from 70 to 322 μS cm^{-1} (Table 2; mean = 147 ± 66 μS cm^{-1}) during MON, 166 to 621 μS cm^{-1} (275 ± 133 μS cm^{-1}) during POM and 137 to 855 μS cm^{-1} (290 ± 192 μS cm^{-1}) during PRM. Similar to EC, TDS also exhibits relatively high values during PRM (Table 2; 88–540 mg L^{-1}) and low during MON (47–204 mg L^{-1}). Gaillardet et al. (1999) emphasized that majority of the world rivers have TDS less than 500 mg L^{-1} and the exceptions are a result of either pollution (i.e., anthropogenic interferences) or aridity (i.e., climate). However, several studies showed that small rivers in tropical mountainous regions have relatively very lower TDS values (i.e., less than 100 mg L^{-1}; e.g., Lewis et al., 1987; McDowell et al., 1995; Harmon et al., 2009). Despite the setting in a tropical mountainous region, relatively higher TDS values in PRB are mainly a result of both semi-arid climate (in the downstream area) and anthropogenic activities (in the upstream segment). Even though humid upstream portion of PRB is dominantly covered by plantations and farmlands, mean TDS has only a range of 70–130 mg L^{-1} (Fig. 2). On the other hand, TDS of semi-arid downstream segment varies between 116 and 249 mg L^{-1}.

Among major cations, Ca^{2+}, Mg^{2+} and Na^+ show relatively higher temporal variability compared to K^+ (Table 2). Ca^{2+} in the river water ranges from 3.36 to 10.09 mg L^{-1} during MON, 6.73–21.87 mg L^{-1} during POM and PRM, while Mg^{2+} concentration varies between 0.73 and 15.47 mg L^{-1} during MON, 3.56 and 12.05 mg L^{-1} during POM and 5.56 and 19.86 mg L^{-1} during PRM (Table 2). Ca^{2+} in river water is mainly controlled by weathering of various silicate minerals as well as by reactions in the carbonate system (Magaritz et al., 1989). Major natural sources of Ca^{2+} in PRB are weathering of chain silicates (pyroxenes and amphiboles) and plagioclase feldspars as well as dissolution of carbonate minerals (e.g., nodular $CaCO_3$). Mg^{2+} in the stream waters is supplied by weathering of ferromagnesian minerals, including pyroxenes and amphiboles as well as dark coloured micas (e.g., biotite), which are abundant in the host lithology (Fig. 3). In addition, Na^+ content in PRB ranges from 1.25 to 26.01 mg L^{-1} during MON, 2.09 to 50.81 mg L^{-1} during POM and 1.44 to 46.04 mg L^{-1} during PRM

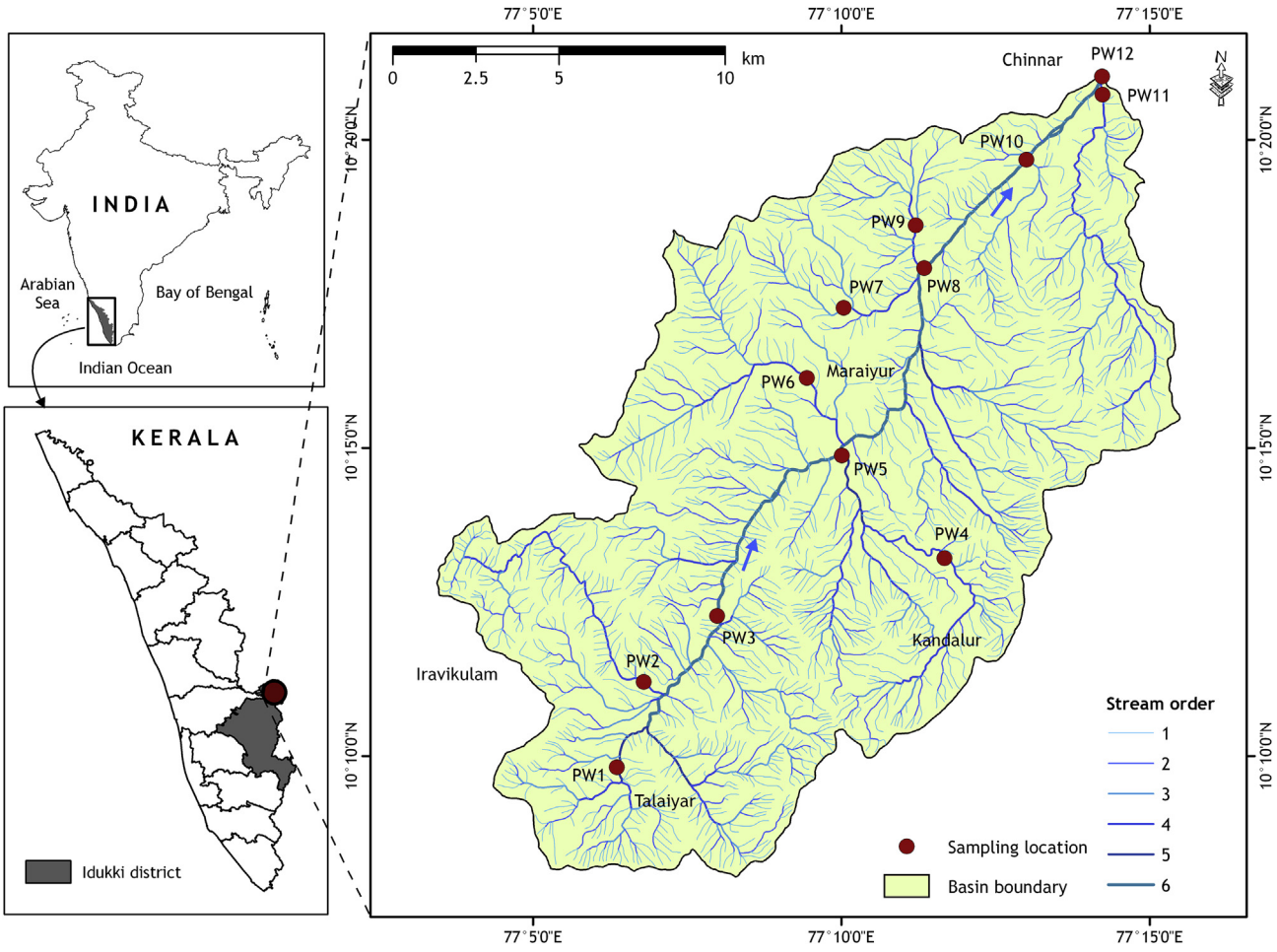

Fig. 1. Location map of Pambar River Basin (PRB). Stream network is delineated from Survey of India topographic maps of 1:50,000 scale. Brown solid circles indicate the river locations sampled during monsoon (MON), post-monsoon (POM) and pre-monsoon (PRM). (For interpretation of the references to color in this figure legend, the reader is referred to the web version of this article.)

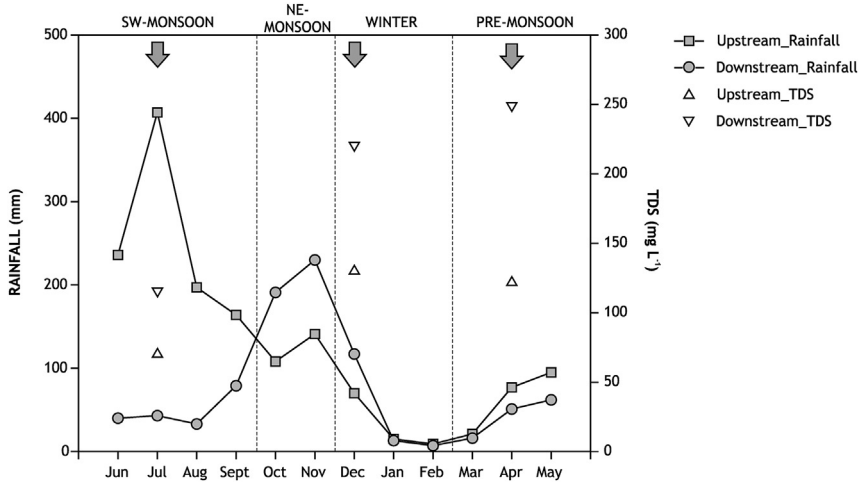

Fig. 2. Mean monthly variation of rainfall (period = 1992–2008) and mean TDS values of different sampling periods, viz., monsoon (MON), post-monsoon (POM) and pre-monsoon (PRM) in the upstream and downstream segments of PRB. Inverted arrows indicate the time of collection of the samples. MON, POM and PRM samples were taken during July, December and April respectively.

(Table 2) and dominant sources of Na^+ in natural system are silicate weathering (predominantly plagioclase), dissolution of evaporitic deposits and atmospheric inputs. K^+ in water is mainly derived by the chemical weathering of K-feldspar (orthoclase and microcline). However, the cations in PRB might also be derived from various anthropogenic activities in PRB (e.g., fertilizer residues from

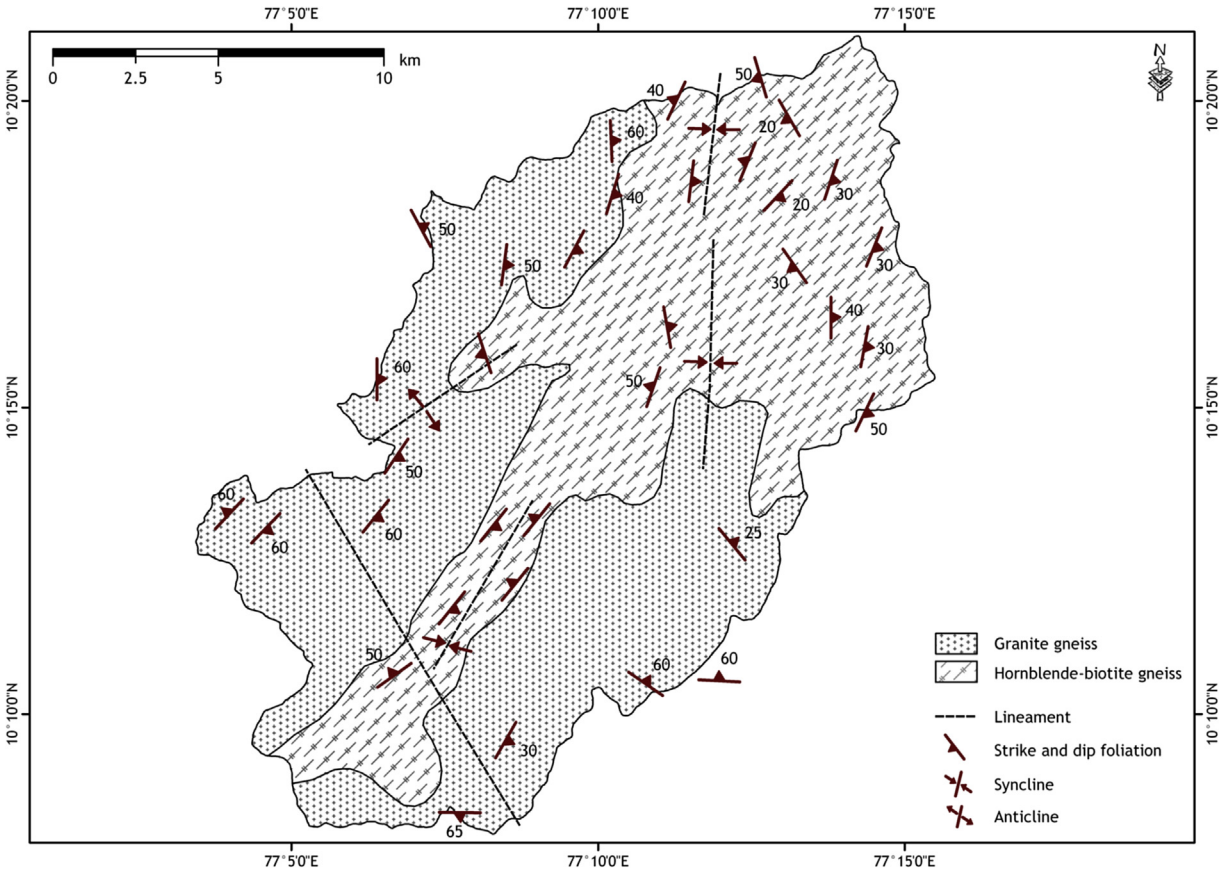

Fig. 3. Geological map of PRB (after GSI, 1992).

Table 1
Environmental characterization of river water sampling stations of PRB.

Sample-ID	Station name	Latitude (N)	Longitude (E)	Location	Elevation (m above msl)	Riparian land use
PW1	Talaiyar	10° 09′ 49″	77° 06′ 21″	Main stream	1428	Tea, Forest
PW2	Lackkam	10° 11′ 13″	77° 06′ 48″	Tributary	1300	Tea
PW3	Chattamunnar	10° 12′ 13″	77° 07′ 59″	Main stream	1120	Tea, Forest
PW4	Kandalur	10° 13′ 13″	77° 11′ 41″	Tributary	1416	Agriculture, Mixed
PW5	Kovilkadavu	10° 14′ 53″	77° 10′ 41″	Tributary	900	Agriculture, Mixed
PW6	Meladi	10° 16′ 08″	77° 09′ 26″	Tributary	980	Agriculture, Mixed
PW7	Karumutti	10° 17′ 17″	77° 10′ 02″	Tributary	967	Forest
PW8	Duvanam	10° 17′ 55″	77° 11′ 21″	Main stream	620	Forest
PW9	Alampatti	10° 18′ 37″	77° 11′ 12″	Tributary	760	Forest
PW10	Champakkad	10° 19′ 41″	77° 13′ 00″	Main stream	460	Forest
PW11	Atti Odai	10° 20′ 44″	77° 14′ 14″	Tributary	450	Forest
PW12	Kootar	10° 21′ 02″	77° 14′ 13″	Main stream	440	Forest

farmlands and plantations, domestic sewage from settlement clusters).

HCO_3^- and Cl^- are the dominant anions in the water samples of PRB, whereas SO_4^{2-} has only secondary significance (Table 2). HCO_3^- concentration has a range from 19.52 to 107.36, 48.80 to 195.20 and 34.16 to 283.04 mg L^{-1} during MON, POM and PRM respectively (Table 2), while Cl^- content varies from 8.51 to 19.86 mg L^{-1} (13.24 ± 3.28 mg L^{-1}) during MON, 22.69 to 65.24 mg L^{-1} (38.06 ± 12.30 mg L^{-1}) during POM and 25.53 to 90.91 mg L^{-1} (40.67 ± 17.54 mg L^{-1}) during PRM. Dominant sources of Cl^- in river water are contribution from cyclic salts, soil salt dissolution (Stallard and Edmond, 1981) as well as anthropogenic inputs (agricultural, industrial and domestic activities). However, HCO_3^- in river water is predominantly derived from silicate and carbonate weathering reactions (e.g., Eqs. (2)–(5); after Mortatti and Probst, 2003).

- Albite into kaolinite:

$$2NaAlSi_3O_8 + 2CO_2 + 11H_2O \rightarrow Al_2Si_2O_5(OH)_4 + 2HCO_3^- + 2Na^+ + 4H_4SiO_4 \quad (2)$$

- K-feldspar into montmorillonite:

$$2KAlSi_3O_8 + 2CO_2 + 6H_2O \rightarrow Al_2Si_4O_{10}(OH)_2 + 2HCO_3^- + 2K^+ + 2H_4SiO_4 \quad (3)$$

- Ca-plagioclase into kaolinite:

Table 2
Summary statistics of the hydrochemistry data for the monsoon (MON), post-monsoon (POM) and pre-monsoon (PRM) sampling in PRB. Grand mean is estimated as the mean of the three sampling seasons.

Season	Parameters Unit	pH	EC $\mu S\ cm^{-1}$	TDS $mg\ L^{-1}$	TSS $mg\ L^{-1}$	TH $mg\ L^{-1}$	TA $mg\ L^{-1}$	Ca^{2+} $mg\ L^{-1}$	Mg^{2+} $mg\ L^{-1}$	Na^{+} $mg\ L^{-1}$	K^{+} $mg\ L^{-1}$	Cl^{-} $mg\ L^{-1}$	SO_4^{2-} $mg\ L^{-1}$	HCO_3^{-} $mg\ L^{-1}$	Si $mg\ L^{-1}$
MON	Mean	7.20	147	93	12.65	36	37	6.03	5.11	8.03	1.75	13.24	3.41	45.14	2.92
	SD	0.23	66	42	3.11	20	19	2.32	4.41	7.49	0.43	3.28	2.37	23.46	1.04
	Min	6.75	70	47	8.04	16	16	3.36	0.73	1.25	1.21	8.51	0.16	19.52	1.35
	Max	7.55	322	204	18.48	76	88	10.09	15.47	26.01	2.72	19.86	6.90	107.36	4.65
POM	Mean	7.11	275	175	16.25	54	69	10.51	6.77	13.45	2.00	38.06	4.25	83.77	3.48
	SD	0.34	133	84	5.40	20	36	3.94	3.11	13.13	0.61	12.30	2.37	44.43	1.57
	Min	6.54	166	104	10.81	32	40	6.73	3.56	2.09	1.08	22.69	0.64	48.80	1.55
	Max	7.70	621	394	28.43	104	160	21.87	12.05	50.81	2.99	65.24	7.70	195.20	6.78
PRM	Mean	7.15	290	186	15.04	66	70	12.47	8.42	10.13	1.89	40.67	6.53	85.40	3.60
	SD	0.31	192	121	5.34	25	56	4.02	3.85	12.27	0.85	17.54	3.03	68.02	1.37
	Min	6.45	137	88	9.49	40	28	6.73	5.56	1.44	0.59	25.53	1.93	34.16	1.55
	Max	7.63	855	540	26.52	136	232	21.87	19.86	46.04	3.94	90.91	11.39	283.04	6.12
Grand mean		7.15	237	151	14.64	52	59	9.67	6.77	10.54	1.88	30.66	4.73	71.44	3.33
WHO (2011)		6.50–8.50	1500	1000		500		100	50	200		250	250	600	

EC-electrical conductivity; TDS-total dissolved solids; TSS-total suspended solids; TH-total hardness; TA-total alkalinity; Si-dissolved silica.

$$CaAl_2Si_2O_8 + 2CO_2 + 3H_2O \rightarrow Al_2Si_2O_5(OH)_4 + 2HCO_3^- + Ca^{2+} + 4H_4SiO_4 \quad (4)$$

- Calcite dissolution:

$$CaCO_3 + CO_2 + H_2O \rightarrow Ca^{2+} + 2HCO_3^- \quad (5)$$

In the hydrochemical system examined, the general cation abundance (in $\mu eq\ L^{-1}$) during MON, POM and PRM is in the order $Mg^{2+} > Na^{+} > Ca^{2+} > K^{+}$, $Na^{+} > Mg^{2+} > Ca^{2+} > K^{+}$ and $Mg^{2+} > Ca^{2+} > Na^{+} > K^{+}$ respectively. However, remarkable differences exist in the relative abundance of cations between the upstream and downstream samples of PRB, i.e., upstream samples follow the order of abundance: $Ca^{2+} > Mg^{2+} > Na^{+} > K^{+}$, while downstream water samples have the order: $Na^{+} > Mg^{2+} > Ca^{2+} > K^{+}$, implying spatial variability in various hydrochemical drivers between the upstream and downstream segments. But, relative abundance of anions is in the order: $HCO_3^- > Cl^- > SO_4^{2-}$ during all the sampling seasons and hardly any differences exists between the upstream and downstream segments. In PRB, the range of Si is between 1.35 and 4.65 $mg\ L^{-1}$ during MON, 1.55 and 6.78 $mg\ L^{-1}$ during POM and 1.55 and 6.12 $mg\ L^{-1}$ during PRM (Table 2).

Table 2 suggests marked temporal variation for various hydrochemical attributes (except for pH and K^{+}) and the parameters tend to display minimum concentrations during MON, suggesting an enhanced dilution due to monsoon rainfall mostly occurring in the upstream portion of PRB (Fig. 2). PRM samples show significantly higher ionic concentrations, compared to MON samples (Table 2; $p \leqslant 0.05$). This temporal variability in PRB can be explained as a result of the variation in rainfall (see Fig. 2) as well as changes in hydrologic pathways, i.e., discharge of the rivers draining the southern Western Ghats during monsoon is predominantly contributed by rainfall as well as surface/subsurface runoff. But, during non-monsoon season, discharge in these rivers is largely contributed by the groundwater system. Even though a relative enrichment (or saturation) of dissolved ions in river water is expected during PRM (compared to POM), the difference in the ionic concentration between POM and PRM is meager, which is mainly due to the unexpectedly higher quantity of summer rainfall (in 2008) occurred in the region.

Although a temporal variability in river water chemistry exists in PRB, there are substantial overlaps in minimum and maximum values between the sampling seasons. In addition, most of the parameters show large values of standard deviation during all the seasons (Table 2). This is primarily because of the contrasting hydrochemical behaviour between the upstream and downstream segments of PRB, i.e., upstream samples are more diluted compared to downstream samples, which is true for all the sampling seasons. The enrichment in the TDS load (i.e., MON → POM → PRM) can be observed in both upstream and downstream samples. For example, the minimum and maximum values of TDS during MON are 47 and 204 $mg\ L^{-1}$ (Table 2; representing locations PW2 and PW11 respectively). During POM, the minimum and maximum values are 104 and 394 $mg\ L^{-1}$ (PW2 and PW11 respectively) and during PRM, the range of TDS is between 88 and 540 $mg\ L^{-1}$ (PW2 and PW11 respectively). Fig. 2 shows the relationship between TDS and rainfall of upstream and downstream segments of PRB. However, the temporal trends of TDS of upstream and downstream are markedly different.

Since climate of the upstream and downstream regions of PRB displays a bipolarity (i.e., humid or tropical-wet-and-dry upstream vs. semi-arid downstream), we hypothesized that significant differences exist in the processes controlling hydrochemistry between the upstream and downstream segments. Hence, chemical composition of river water samples between upstream (PW1–PW6) and downstream (PW7–PW12) regions is compared (Fig. 4). Fig. 4 implies that the concentration of most of the hydrochemical attributes in the downstream samples is significantly higher ($p \leqslant 0.05$), compared to the upstream samples. Supply of the highly "mineralized" waters (i.e., with higher dissolved constituents) of the semi-arid segments of the basin has a significant role in the elevated dissolved load of the downstream samples.

3.2. Sources and processes controlling solute chemistry

As a considerable amount of the dissolved load (mainly Ca^{2+}, Mg^{2+}, Na^{+}, K^{+} and SO_4^{2-}) in rivers is derived from the atmosphere (via. rainfall, dry deposition, etc.), the constituents need to be corrected for cyclic-salt inputs (Stallard and Edmond, 1981, 1983). The cyclic-salt correction provides further insights to the magnitude of the atmospheric inputs into the river system as well as the geogenic

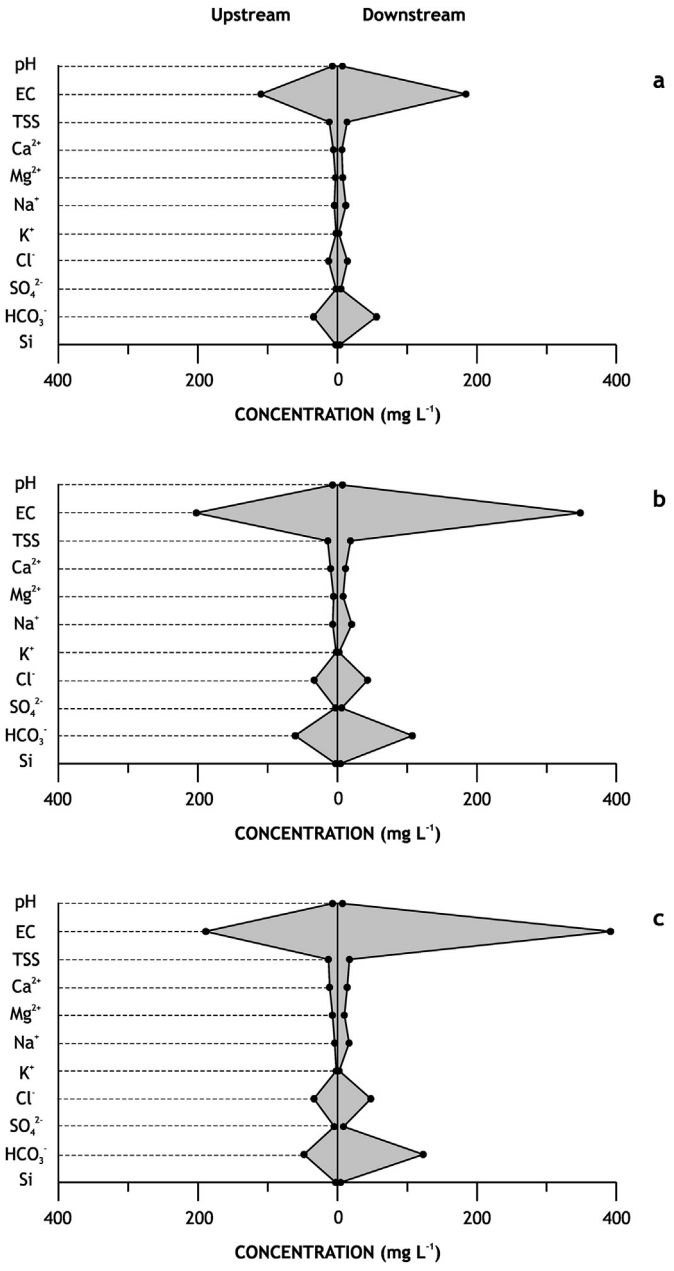

Fig. 4. Spatial variation of various hydrochemical attributes between upstream and downstream segments of PRB during (a) monsoon, MON, (b) post-monsoon, POM and (c) pre-monsoon, PRM sampling periods.

and anthropogenic contributions. Hence, in PRB, major cations and SO_4^{2-} during MON were corrected for atmospheric inputs following the methodology of Murphy and Stallard (2012). In PRB, SO_4^{2-} (~85%) is mainly contributed by atmospheric processes, followed by Na^+ (~50%), whereas K^+ and Mg^{2+} receive a contribution of about 15–25% respectively. However, Ca^{2+} receives only a minor share (~5%) from atmospheric contributions. Except for Ca^{2+} and K^+, upstream samples have comparatively higher atmospheric contribution compared to downstream samples. The contribution of cyclic salts to riverine dissolved salt loads is expected to decrease with increasing distance from the sea (Stallard and Edmond, 1981). But, in (east-flowing) Pambar, the upstream portion of the basin is closer to the Arabian Sea (see Fig. 1), which may be the reason for the relatively higher contributions from atmospheric inputs.

Relatively higher molar ratios between Cl^- and Na^+ (>1.0; Table 3) clearly indicate multiple sources of origin for these ions (i.e., Na^+ from weathering and atmospheric inputs), while Cl^- from atmospheric deposition, dissolution of soil salts as well as anthropogenic inputs. Peters and Ratcliffe (1998) reported derivation of Cl^- from rainwater and then concentrated as the result of evaporation within the shallow soil horizon. Trace Cl^- (for OH^-) in amphibole minerals in the rocks of the watersheds is also a minor, natural source (Buell and Peters, 1988). The upstream samples of PRB has considerably higher Cl^-/Na^+ ratios compared to downstream samples, which can be explained by the differences in the degree of anthropogenic disturbances as well as the variation in atmospheric inputs.

Among various natural processes controlling hydrochemistry of rivers, rock weathering and mineral dissolution play an important role in PRB, which is illustrated in the Gibbs (1970) model depicting the magnitude of various processes determining the chemical composition of surface water (Fig. 5). However, noticeable differences exist between the upstream and downstream water samples, i.e., relatively high TDS (116, 221 and 249 mg L^{-1} respectively during MON, POM and PRM) and $Na^+/Na^+ + Ca^{2+}$ values (0.60 during MON and POM and 0.49 during PRM) characterize the downstream waters, whereas low TDS (70, 130 and 122 mg L^{-1} respectively during MON, POM and PRM) and $Na^+/Na^+ + Ca^{2+}$ values (0.42, 0.40 and 0.25 respectively during MON, POM and PRM) portray the upstream waters. According to Gibbs (1970), as the Ca^{2+}/Na^+ increases, the interaction between water and rock/soil increases (such as in the upstream samples), while evaporation decreases the ratio due to precipitation of calcite which removes Ca^{2+} from the water (in the downstream samples). Among various seasons, MON has comparatively low TDS and $Na^+/Na^+ + Ca^{2+}$ values, while PRM shows high values, implying the significance of monsoon rainfall in the hydrochemistry of PRB. In addition, the trend of downstream variation of hydrochemistry is parallel to the saturation trend (Fig. 5), which also indicates the significance of

Table 3
Various ionic ratios (used in this study) for the monsoon (MON), post-monsoon (POM) and pre-monsoon (PRM) samples in PRB.

Ionic ratio	Upstream (PW1–PW6)			Downstream (PW7–PW12)			Total		
	MON	POM	PRM	MON	POM	PRM	MON	POM	PRM
[b]Cl^-/Na^+	2.63 (1.32–7.36)	4.07 (1.96–9.68)	6.41 (4.42–11.50)	1.10 (0.35–1.85)	1.69 (0.83–2.45)	2.46 (1.28–3.73)	1.86	2.88	4.43
[a]$Si/Na^+ + K^+$	0.48 (0.18–0.81)	0.36 (0.19–0.60)	0.58 (0.31–0.83)	0.36 (0.14–0.62)	0.23 (0.12–0.34)	0.34 (0.10–0.47)	0.42	0.30	0.46
[a]$Ca^{2+} + Mg^{2+}/Na^+ + K^+$	2.31 (1.47–3.17)	3.25 (1.91–6.76)	6.34 (4.08–12.36)	2.15 (1.07–4.64)	1.56 (0.91–2.32)	2.45 (1.32–3.95)	2.23	2.41	4.40
[b]HCO_3^-/Ca^{2+}	4.47 (2.38–8.59)	4.28 (3.00–6.19)	2.83 (2.22–3.54)	5.71 (3.81–8.89)	6.21 (4.36–9.53)	5.68 (3.43–8.50)	5.09	5.25	4.25
[a]$Ca^{2+} + Mg^{2+}/HCO_3^-$	0.96 (0.44–1.60)	0.97 (0.62–1.60)	1.50 (1.08–2.00)	1.18 (0.60–2.72)	0.74 (0.60–0.94)	0.81 (0.59–1.06)	1.07	0.86	1.16
[a]K^+/Na^+	0.33 (0.13–0.87)	0.16 (0.10–0.30)	0.25 (0.19–0.33)	0.12 (0.05–0.19)	0.09 (0.03–0.13)	0.11 (0.03–0.21)	0.22	0.13	0.18
[a]$HCO_3^-/HCO_3^- + SO_4^{2-}$	0.94 (0.82–0.99)	0.95 (0.90–0.98)	0.90 (0.86–0.95)	0.88 (0.80–0.97)	0.92 (0.87–0.97)	0.90 (0.85–0.96)	0.91	0.94	0.90
[a]Ca^{2+}/SO_4^{2-}	26.81 (2.39–75.65)	15.57 (4.02–31.49)	7.24 (4.00–14.62)	3.59 (1.75–7.93)	5.09 (2.58–11.67)	3.94 (2.48–6.28)	15.20	10.33	5.59

Values expressed as mean and range (in parentheses).
[a] Ratios derived from μeq values.
[b] Ratios derived from μmolar concentrations.

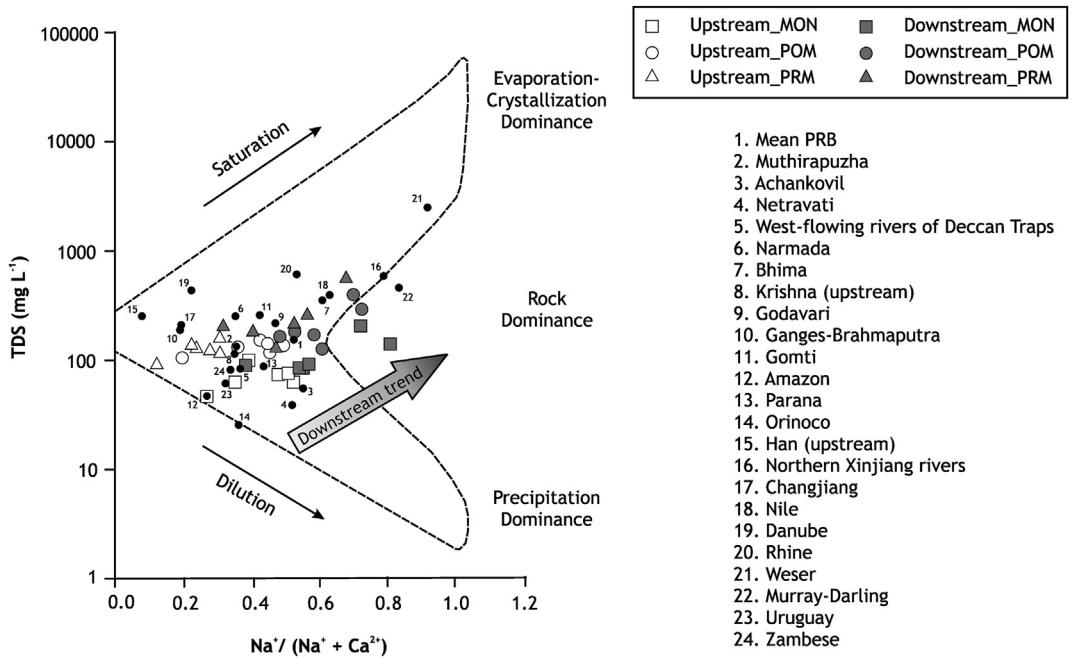

Fig. 5. Hydrochemistry data of PRB during monsoon (MON), post-monsoon (POM) and pre-monsoon (PRM) sampling in Gibbs (1970) plot, a diagrammatic representation of processes controlling chemistry of surface waters. Shaded block arrow indicates the downstream trend of the hydrochemistry data. Hydrochemistry data from Galy and France-Lanord (1999), Gaillardet et al. (1999), Chen et al. (2002), Mortatti and Probst (2003), Singh et al. (2004), Das et al. (2005), Prasad and Ramanathan (2005), Li and Zhang (2008), Jha et al. (2009), Gupta et al. (2011), Zhu et al. (2011), Gurumurthy et al. (2012), and Thomas et al. (2014) for comparison.

evaporation–crystallization processes in the downstream hydrochemistry. In Mg^{2+}/Na^{+} vs. Mg^{2+}/Ca^{2+} plot (Fig. 6), water samples of PRB show considerable differences between upstream and downstream regions. The upstream samples are characterized by lower range of Mg^{2+}/Ca^{2+} ratios and variable Mg^{2+}/Na^{+} ratios, implying evidences of rock–water interaction. However, the downstream samples have relatively higher Mg^{2+}/Ca^{2+} ratios and varying Mg^{2+}/Na^{+} ratios, which also suggest the significance of evaporation process along with rock–water interaction in downstream hydrochemistry.

The Na^{+}-normalized Ca^{2+} vs. Mg^{2+} and Na^{+}-normalized Ca^{2+} vs. HCO_3^{-} plots (Fig. 7a and b; after Gaillardet et al., 1999) indicate that PRB waters are influenced by rock–water interaction, mainly by silicate weathering and carbonate dissolution. Even though PRB is underlain by silicate rocks (e.g., granite gneiss, hornblende-biotite-gneiss), nodular $CaCO_3$ is present in the subsurface soil profiles (29–99 cm) of the semi-arid segment (SSO, 2007), which is a major source of carbonates. Meybeck (1987) concluded that carbonates weather 12–40 times more easily when compared to silicates, and hence, a very small patch of carbonate bed can have a greater control on the regional water chemistry. Fig. 7a and b also imply that the sample poles fall parallel to the trend line between

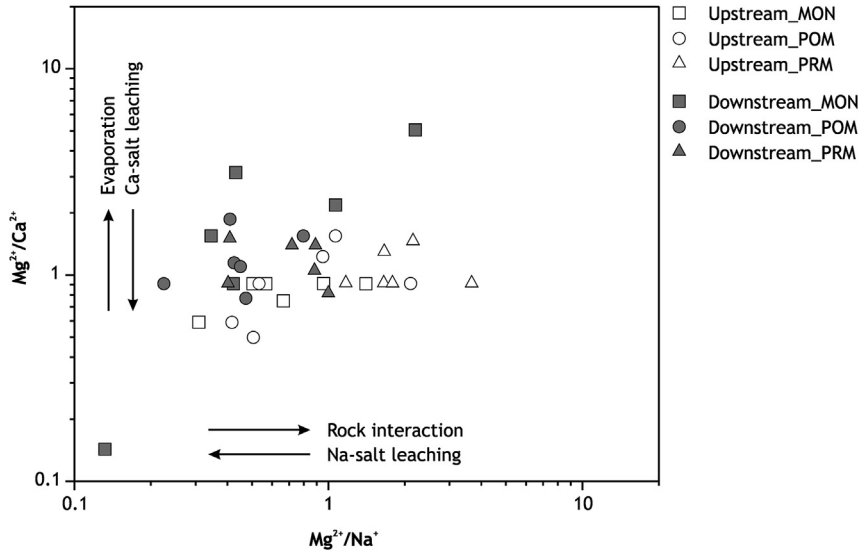

Fig. 6. Bivariate plot of Mg^{2+}/Ca^{2+} vs. Mg^{2+}/Na^{+} molar ratios (after Zhu et al. (2011)). The plot enables discrimination between upstream (open symbols) and downstream (shaded symbols) samples during monsoon (MON), post-monsoon (POM) and pre-monsoon (PRM).

silicate and carbonate domains, which can be inferred as possible mixing between silicate and carbonate end members. In addition, the contribution by dissolution of soil evaporites (during MON and POM) is also evidenced by relatively lower Ca^{2+}/Na^{+} ratios (e.g., semi-arid, downstream samples such as PW9 and PW11; Fig. 7a).

Mean $Si/Na^{+} + K^{+}$ ratios during MON, POM and PRM are 0.42, 0.30 and 0.46 respectively (Table 3), which also reaffirm the role of silicate weathering. However, comparatively lower ratios during MON and POM (compared to PRM; Table 3), due to additional inputs of Na^{+} and K^{+}, suggest mixing of dissolved load from sources other than weathering (e.g., atmospheric inputs, dissolution of soil evaporites, anthropogenic activities). Mean $Si/Na^{+} + K^{+}$ ratios of upstream samples during MON, POM and PRM are 0.48, 0.36 and 0.58 respectively (Table 3), whereas downstream samples show relatively lower ratios (i.e., 0.36, 0.23 and 0.34 during MON, POM and PRM respectively), implying intense silicate weathering in the humid upstream region. $Ca^{2+} + Mg^{2+}/Na^{+} + K^{+}$ ratios during MON, POM and PRM are 2.23, 2.41 and 4.40 respectively (Table 3), which also suggest multiple sources controlling hydrochemistry of PRB. Moreover, upstream samples can be discriminated from downstream samples by relatively higher $Ca^{2+} + Mg^{2+}/Na^{+} + K^{+}$ ratios (Table 3). In upstream samples, $Ca^{2+} + Mg^{2+}/Na^{+} + K^{+}$ ratios are relatively low during MON, whereas in downstream areas low values are recorded during POM (Table 3), i.e., the periods of relatively high rainfall (see Fig. 2). Such low ratios can be explained by higher contribution by atmospheric processes as well as dissolution of soil evaporites.

Mean molar ratios of HCO_3^- to Ca^{2+} during MON, POM and PRM are 5.09, 5.25 and 4.25 respectively (Table 3), but upstream and downstream samples show substantial differences. Upstream samples are characterized by relatively lower HCO_3^-/Ca^{2+} ratios during the sampling seasons (4.47, 4.28 and 2.83 for MON, POM and PRM respectively; Table 3), while downstream samples have much higher values (5.71, 6.21 and 5.68 for MON, POM and PRM respectively). Moreover, the ratios during MON and POM are comparably larger (due to higher concentration of HCO_3^-) than that of PRM, which might be a result of the dissolution of atmospheric CO_2 during the monsoon rains. A positive linear relationship of HCO_3^- with Ca^{2+} and Mg^{2+} (Fig. 8) can be attributed to their common source, and in general, Ca^{2+} and Mg^{2+} ions are balanced by HCO_3^- ions (mean $Ca^{2+} + Mg^{2+}/HCO_3^- = 1.07$, 0.86 and 1.16 respectively during MON, POM and PRM; Table 3). However, downstream samples show significant deviation from the 1:1 equiline toward the HCO_3^- axis, indicating a relative enrichment of HCO_3^- ions and the excess HCO_3^- is balanced by other ions such as Na^{+} and K^{+} ($r = 0.91$ and 0.51 respectively; Table 4).

Mean K^{+}/Na^{+} ratios during MON, POM and PRM are 0.22, 0.13 and 0.18 respectively (Table 3), indicating that PRB waters are very sodic ($K^{+}/Na^{+} < 0.40$). On comparison between upstream and downstream water samples, upstream samples have significantly high K^{+}/Na^{+} ratios (0.33, 0.16 and 0.25 during MON, POM and PRM respectively; $p \leqslant 0.05$), compared to downstream samples (0.12, 0.09 and 0.11 during MON, POM and PRM respectively). Such a difference between upstream and downstream samples can be inferred as less intense weathering in the downstream region (that

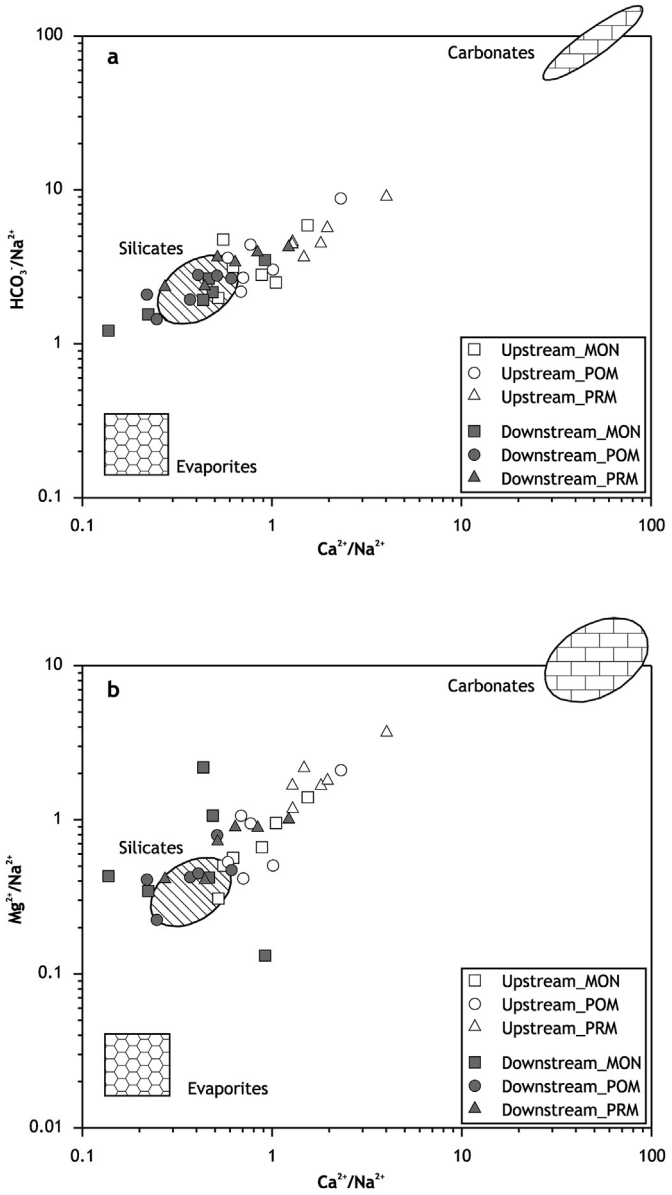

Fig. 7. Mixing diagrams using Na-normalized molar ratios in the water samples during monsoon (MON), post-monsoon (POM) and pre-monsoon (PRM) in PRB. The data of three main end member reservoirs (evaporite dissolution, silicate weathering and carbonate dissolution) were obtained after Gaillardet et al. (1999).

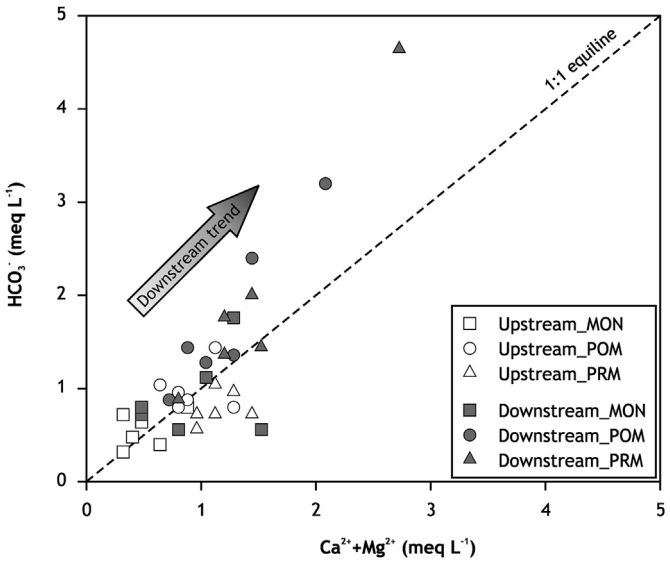

Fig. 8. Bivariate plot of $Ca^{2+} + Mg^{2+}$ vs. HCO_3^- during monsoon (MON), post-monsoon (POM) and pre-monsoon (PRM) sampling in PRB. Shaded block arrow points the downstream trend. Analytical data of upstream samples are clustered along the 1:1 line, while downstream data show considerable deviations from the equiline.

is not enough to dissolve the resistant K-feldspars to a great extent). However, higher concentration of K^+ of the upstream waters can also be derived from anthropogenic sources such as fertilizer residues (e.g., potash).

The ratio of HCO_3^- to $HCO_3^- + SO_4^{2-}$ is used to characterize the relative importance of two major proton-producing reactions: carbonization and oxidation of sulfides (Prasad and Ramanathan, 2005). The ratios of HCO_3^- to $HCO_3^- + SO_4^{2-}$ in PRB (0.91 during MON, 0.94 during POM and 0.90 during PRM; Table 3) are closer to 1.0, suggesting the occurrence of carbonization reaction involving dissolution and acid hydrolysis, which draws protons from atmospheric inputs and is further confirmed by relatively higher Ca^{2+}/SO_4^{2-} ratios (i.e., 15.20, 10.33 and 5.59 during MON, POM and PRM respectively; Table 3). It is noteworthy that Ca^{2+}/SO_4^{2-} ratios also show remarkable differences between upstream and downstream regions, i.e., relatively lower values in downstream compared to upstream areas (Table 3). The lower ratios in the downstream samples amply reflect the significance of SO_4^{2-} in the semi-arid, downstream areas, probably derived from leaching of soil salts (e.g., $CaSO_4$).

3.3. Characterization of hydrochemical facies

The chemical composition of river water of PRB is also explained by plotting the major cations and anions in the Piper (1944) diagram (Fig. 9). The dominant cation facies during MON, POM and PRM are principally mixed type or 'no dominant type', while the dominant anion facies is HCO_3 type. In the diagram, the water samples are dispersed on both sides of the HCO_3–Cl line. The downstream samples are more enriched in HCO_3 compared to the upstream samples, suggesting the vital role of groundwater-dominating discharge in the downstream hydrochemistry. Frazee (1982) developed a specialized interpretive water classification and later Upchurch (1992) suggested a descriptive classification of natural waters based on Piper diagram and both the schemes are used in this study to interpret the hydrochemical facies in PRB. Accordingly, the dominant water types of PRB are mixed cation–HCO_3 followed by mixed cation–HCO_3–Cl during MON, mixed cation–HCO_3–Cl during POM and Ca–Mg–HCO_3–Cl during PRM.

Mixed cation–HCO_3–Cl waters are considered as "transitional waters", where these water types refer to waters that are evolving by geochemical reactions with bedrock as well as soil-matrix or waters that changed their geochemical character by mixing with other geochemically distinct waters (Frazee, 1982). Further, these waters are the product of mixing among two or more end members. Similar to mixed cation–HCO_3–Cl waters, Ca–Mg–HCO_3–Cl waters are also "transitional waters", but Na^+ has less significance. Mixed cation–HCO_3 waters, showing dominance in PRB during MON (as well as subsidiary role in other seasons), might be derived from the interaction of "fresh recharge waters" (Ca–Na–HCO_3 type) with Mg-rich minerals in the host rocks (e.g., hornblende-biotite gneiss). In PRB, mixed cation–HCO_3 water samples were collected from locations, viz., PW4, PW5, PW6, PW7 and PW11, where the lithology is hornblende-biotite gneiss (Fig. 3). The water types between the upstream and downstream segments of PRB also show distinctiveness in the Piper diagram, i.e., a general downstream trend from Cl apex to HCO_3 apex is apparent during all the sampling seasons (Fig. 9). This trend suggests a spatial discrimination (in PRB) between the upstream waters with anthropogenic signatures (samples near to Cl apex) and downstream waters of groundwater-dominating discharge (samples closer to HCO_3 apex).

3.4. Partial pressure of CO_2 (pCO_2)

Partial pressure of CO_2 (pCO_2) for the water samples of MON, POM and PRM was estimated from pH values and HCO_3^- concentrations (Table 5) and the results indicate relatively higher pCO_2 during all the seasons compared to the atmosphere (i.e., $10^{-3.5}$ atm). Mean pCO_2 of stream water in PRB is nearly 10 times the atmospheric pCO_2 during MON, roughly 22 times during POM and about 23 times during PRM. Such supersaturation with respect to atmosphere is a global trend, indicating the disequilibrium existing in natural waterbodies vis-à-vis the atmosphere (Raymahashay, 1986; Anshumali and Ramanathan, 2007). The downstream water samples have relatively higher $pCO_{2\ (river)}/pCO_{2\ (atmosphere)}$ during MON and PRM (mean = 12.27 and 29.23 respectively) compared to the upstream samples (mean = 6.88 and 15.06 respectively), implying the significant discharge contribution from aquifers. However, downstream samples have comparatively lower $pCO_{2\ (river)}/pCO_{2\ (atmosphere)}$ during POM, which could be attributed to the comparatively higher quantity of rainfall (see Fig. 2). In addition, lower $pCO_{2\ (river)}/pCO_{2\ (atmosphere)}$ ratios are related with high rainfall episodes in both upstream and downstream segments. Similarly, Thomas et al. (2014) also reported relatively smaller $pCO_{2\ (river)}/pCO_{2\ (atmosphere)}$ ratios (in a tropical mountainous river basin of the southern Western Ghats) associated with monsoon rainfall and significantly larger ratios during non-monsoon season due to groundwater-dominating discharge.

3.5. Downstream trend of hydrochemical variability

Since the climate of PRB gradually varies downstream (i.e., humid upstream to semi-arid downstream), the trends of downstream variation of selected hydrochemical attributes were assessed by curve fitting. The best-fit curve model between hydrochemical attributes (as dependent variable) and P_{ma} (as independent variable) effectively indicates the downstream variability of hydrochemistry with respect to the variation in rainfall. Since P_{ma} of each sampling location is not available, this study made use of elevation above msl as a proxy of P_{ma} (because P_{ma} shows a linearly decreasing trend toward lower elevations; Thomas, 2012).

Although rainfall shows a linear (decreasing) trend toward downstream, the best-fit models for selected hydrochemical attributes (e.g., EC, TDS, Na^+ and HCO_3^-) of PRB (Fig. 10) suggest that the downstream hydrochemical variability of this 'allochthonous' river (i.e., rivers originating in humid or sub-humid climate and later flows through semi-arid or arid climate) is strongly non-linear. In PRB, the downstream variability of the hydrochemical attributes follows a power function ($f(x) = ax^k$). The power function curve has two major phases: a slow increase in hydrochemical concentration, followed by a period of rapid increase (Fig. 10). The humid regions (in PRB) are characterized by relatively low values of hydrochemical attributes and the increasing rate of hydrochemical concentration with respect to declining elevation (and hence rainfall) is gradual. However, thereafter an abrupt change is noticed toward the semi-arid segments. Hence, the region where the power function curve changes from the slow and steady increase to the rapid increase (i.e., roughly between 1000 and 800 m above msl) can be considered as the climatic transition zone (i.e., humid to semi-arid) of PRB. Plotting dissolved load against distance to outfall, Lecomte et al. (2005) demonstrated that major cations (Ca^{2+}, Na^+, K^+, and Mg^{2+}) and TDS of Los Reartes river basin ($A = 250\ km^2$), Argentina show an increasing exponential trend toward the downstream direction regardless of the linearly declining downstream trend of P_{ma}. The hydrochemical data in PRB also fit an exponential model (see Fig. 10), but the coefficients of determination (r^2) are slightly smaller than that of the power function model, which is due the downstream sample PW11 (i.e., at elevation 455 m above msl).

Table 4
Correlation matrix of selected hydrochemical attributes in PRB.

	pH	EC	TSS	Ca^{2+}	Mg^{2+}	Na^{+}	K^{+}	Cl^{-}	SO_4^{2-}	HCO_3^{-}	Si
pH	1.00	0.30	0.11	0.26	0.18	0.34*	0.00	0.21	0.20	0.31	0.22
EC		1.00	0.12	0.81**	0.74**	0.91**	0.51**	0.88**	0.50*	0.99**	0.69**
TSS			1.00	0.24	0.15	−0.01	0.21	0.23	0.42*	0.08	0.22
Ca^{2+}				1.00	0.59**	0.66**	0.39*	0.83**	0.43*	0.77**	0.46**
Mg^{2+}					1.00	0.68**	0.38*	0.64**	0.34*	0.71**	0.52**
Na^{+}						1.00	0.51**	0.67**	0.32	0.91**	0.68**
K^{+}							1.00	0.36*	0.24	0.51**	0.52**
Cl^{-}								1.00	0.47**	0.83**	0.52**
SO_4^{2-}									1.00	0.47**	0.47**
HCO_3^{-}										1.00	0.71**
Si											1.00

The values underlined imply strong correlation between the corresponding variables.
* Correlation is significant at the 0.05 level.
** Correlation is significant at the 0.01 level.

3.6. Comparison with other river basins in India and the world

The hydrochemical attributes of PRB (grand mean in Table 2) are compared with selected rivers of the Western Ghats, rivers of the Peninsular India and the rivers draining rain shadow regions of other parts of the world (Table 6). In general, TDS and the dissolved ions are relatively higher in PRB, compared to other rivers draining the Western Ghats with the exception of Periyar and Chalakkudy Rivers. In Table 6, the river basins draining the Western Ghats (except Netravati and the rivers draining Deccan Volcanic Terrain) are developed on crystalline rocks of Archaean to Proterozoic ages with charnockites (charnockite, charnockite gneiss, cordierite gneiss and pyroxene granulite), khondalites (khondalite, quartzite and calc-granulite), migmatites (composite gneisses and schist) and granitoids (GSI, 2005). But, major litho types of Netravati river basin encompass meta-sediments, banded iron formations, amphibolitic facies gneisses and foliated charnockites transformed into pyroxene-bearing granulites (Radhakrishna and Vaidyanadhan, 1997). Dominant lithology of west-flowing rivers of Deccan Volcanic Terrain is Deccan Trap basalts, which are predominantly tholeiitic lavas (Das et al., 2005). The rivers draining the Western Ghats (in Table 6) other than Pambar are west-flowing rivers and most of them have relatively larger basin area, compared to PRB. In addition, these basins experience relatively higher amount of rainfall (2000–5000 mm) and thereby higher discharge, which is attributed to the lower dissolved chemical load. However, lower Si of (semi-arid) PRB compared to the (humid) west-flowing rivers (range = 45–360 μM L^{-1}) implies less intense weathering of silicate minerals as climate and basin hydrology has a significant role in silicate weathering and silicate flux of rivers. Si concentration of the west-flowing rivers of Deccan Volcanic Terrain is relatively very high (360 μM L^{-1}) compared to PRB, suggesting differences in lithology as well as climate. Maya et al. (2007) underscored the vital role of industrialization and urbanization on substantially high dissolved load in Periyar and Chalakkudy Rivers along with seawater intrusion (in the lower reaches). However, hydrochemistry in the upstream areas of both the rivers is predominantly controlled by silicate weathering and agricultural activities in the catchments.

Further, hydrochemistry of PRB is also different from various rivers of the Peninsular India (Table 6). Even though the dominant litho unit of the Peninsular rivers is Deccan Trap basalts, other litho types such as sandstone, shale, limestone of Vindhyan group and Gondwana sediments (in Narmada river basin), Dharwars (phyllites, schists and amphibolites), Archaean (granites and gneisses) as well as Precambrian and Gondwana sedimentary rocks (in Godavari river basin) also constitute the regional geology (Jha et al., 2009; Gupta et al., 2011). The mean annual rainfall of the river basins, viz., Narmada, Bhima, upstream of Krishna and Godavari is 1178, 770, 770 and 923 mm respectively (Das et al., 2005; Jha et al., 2009; Gupta et al., 2011). On comparison with PRB, the Peninsular rivers (Narmada, Bhima and Godavari) have more mineralized waters with dominance of Ca^{2+}, Mg^{2+}, HCO_3^{-} and Si and the variations can be explained by the semi-arid to arid climate as well as lithological differences (i.e., dominance of basalts).

On comparison with Los Reartes River (draining semi-arid regions of the Sierras de Cordoba in the Sierras Pampeanas of Argentina), PRB has relatively higher mineralization and higher dissolved constituents (except Si), which might also be due to the differences in lithology and climate. Major lithologic units of Los Reartes river basin are biotite–muscovite granite, cordierite gneiss, biotite–garnet gneiss and loess-like and fluvial sediments. Even though, the spatial rainfall pattern of the Los Reartes river basin (i.e., >1000 mm in the upstream reaches and 750 mm in the downstream reaches) is more or less similar to that of PRB, low

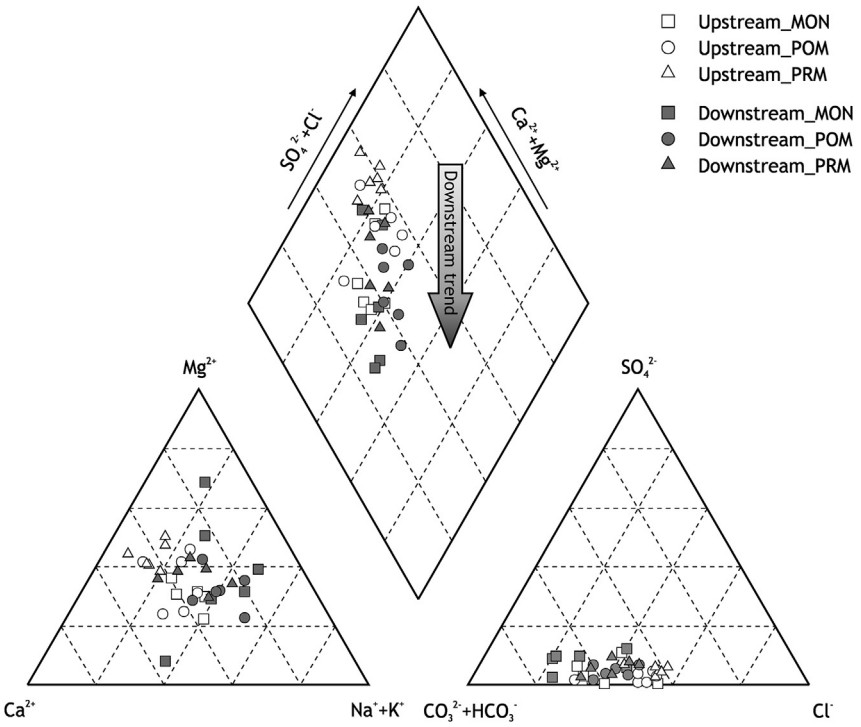

Fig. 9. Piper (1944) diagram comparing hydrochemical compositional variation and showing water types during monsoon (MON), post-monsoon (POM) and pre-monsoon (PRM) sampling in PRB.

Table 5
Log $mHCO_3^-$ and log pCO_2 for the monsoon (MON), post-monsoon (POM) and pre-monsoon (PRM) samples in PRB.

Sample-ID	MON		POM		PRM	
	Log $mHCO_3^-$	Log P_{CO2}	Log $mHCO_3^-$	Log P_{CO2}	Log $mHCO_3^-$	Log P_{CO2}
PW1	−3.32	−2.42	−3.10	−1.96	−3.14	−1.80
PW2	−3.49	−3.12	−3.10	−2.20	−3.25	−2.89
PW3	−3.40	−2.70	−3.06	−2.40	−3.14	−2.61
PW4	−3.19	−2.52	−2.84	−2.21	−3.02	−2.43
PW5	−3.10	−2.60	−3.02	−2.00	−2.98	−2.46
PW6	−3.14	−2.80	−2.98	−2.33	−3.14	−2.53
PW7	−3.14	−2.68	−3.06	−1.80	−3.06	−2.36
PW8	−3.25	−2.61	−2.84	−2.15	−2.75	−1.67
PW9	−2.95	−2.28	−2.62	−2.23	−2.70	−1.95
PW10	−3.10	−2.05	−2.89	−2.34	−2.87	−2.22
PW11	−2.75	−2.51	−2.49	−2.40	−2.33	−1.89
PW12	−3.25	−2.61	−2.87	−2.58	−2.84	−2.68

temperatures, irregular rainfall concentrated in one season and occasional snowfall in winter are typical features of Los Reartes river basin (Lecomte et al., 2005). However, both the basins show marked differences in hydrochemistry between upstream and downstream reaches. In addition, with regard to cations (Ca^{2+}, Na^+, K^+, and Mg^{2+}), concentrations increase in the downstream direction (along with TDS) following an exponential function, while major ions in PRB follows a power function followed by an exponential function. However, hydrochemistry of Hawkesbury-Nepean River, Australia shows relative enrichment of Na^+, Cl^- and SO_4^{2-} with respect to PRB. The spatial variability in rainfall in Hawkesbury-Nepean river basin (~1500 mm in the upstream reaches and 500 mm in the rain shadow plains) is also similar to that of PRB. But, major lithology of the basin is sandstone, shale and a belt of metamorphic and igneous rocks. According to Markich and Brown (1998), major ion composition of the freshwater reaches of the Hawkesbury-Nepean River is predominantly influenced by both sea-salt aerosols in rainwater (in headwaters) and connate sea-salt in groundwater (in mid-lower reaches), which are the reasons for significantly differing hydrochemical compositions.

4. Summary and conclusion

The river water chemistry of Pambar River Basin (PRB), draining a rain shadow region of the southern Western Ghats, was analyzed for three seasons, viz., monsoon (MON), post-monsoon (POM) and pre-monsoon (PRM) to examine the spatio-temporal trends and to understand the major controls on hydrochemistry.

The hydrochemical attributes, except pH and K^+, exhibit distinct temporal variation mainly due to monsoon-driven climatic seasonality. Relative abundance of cations between the upstream and downstream samples of PRB shows notable differences in that the upstream samples follow the order of abundance: $Ca^{2+} > Mg^{2+} > Na^+ > K^+$, while the downstream water samples have the order: $Na^+ > Mg^{2+} > Ca^{2+} > K^+$. However, relative abundance of anions (for both upstream and downstream) is in the

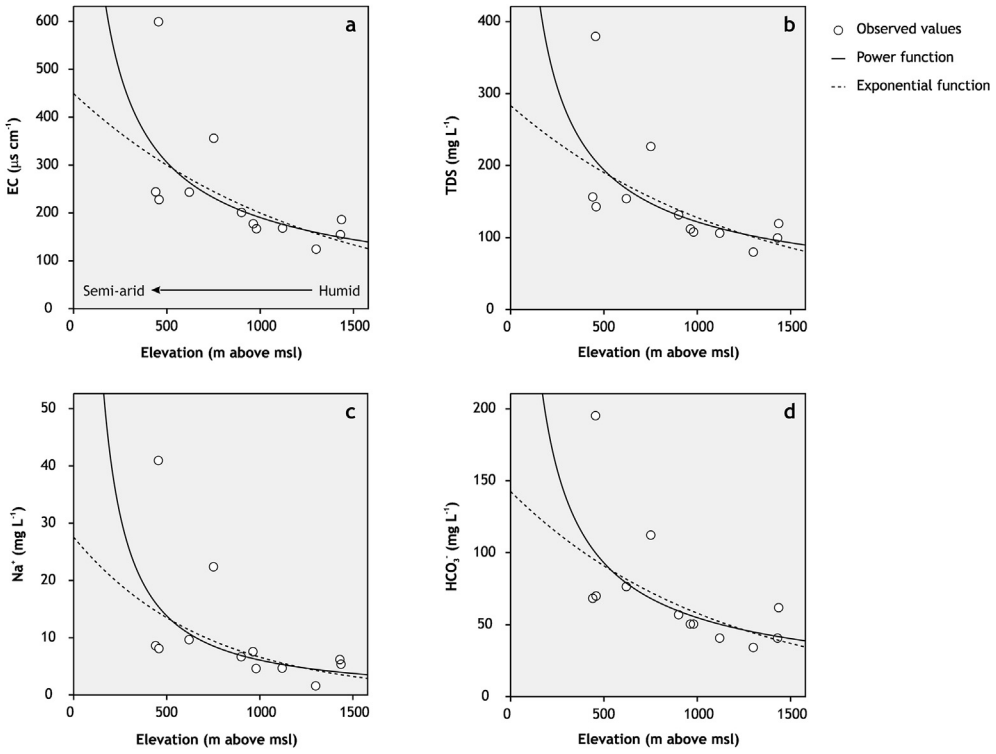

Fig. 10. Downstream concentration trend of (a) EC, (b) TDS, (c) Na^+ and (d) HCO_3^- with lines of best-fit. In PRB, power function (followed by exponential function) explains the downstream hydrochemical variability.

Table 6
Comparison of hydrochemistry of PRB with selected rivers of the Western Ghats, rivers of Peninsular India and rivers draining rain shadow regions of other parts of the world.

River	TDS mg L^{-1}	Ca^{2+} µM L^{-1}	Mg^{2+} µM L^{-1}	Na^+ µM L^{-1}	K^+ µM L^{-1}	Cl^- µM L^{-1}	SO_4^{2-} µM L^{-1}	HCO_3^- µM L^{-1}	Si µM L^{-1}	Reference
Western Ghats Rivers, India										
Pambar	151	241	279	458	48	865	49	1171	35	This study
Muthirapuzha	131	255	213	244	57	1022	39	841	45	Thomas et al. (2014)
Achankovil	54	67	49	142	25	649	6	220	71	Prasad and Ramanathan (2005)
Periyar	636	274	1605	–	–	14,103	573	328	73	Maya et al. (2007)
Chalakkudy	667	324	1646	–	–	14,865	687	295	73	Maya et al. (2007)
Netravati	38	74	53	138	18	91	12	309	195	Gurumurthy et al. (2012)
West-flowing rivers of Deccan Volcanic Province	82	171	132	172	6	110	12	665	360	Das et al. (2005)
Peninsular Rivers, India										
Narmada	248	644	447	609	38	122	30	2748	329	Gupta et al. (2011)
Bhima	347	693	549	1848	45	936	528	2480	380	Das et al. (2005)
Krishna (upstream)	112	296	189	277	14	192	37	991	270	Das et al. (2005)
Godavari	214	778	438	1193	100	720	188	2252	438	Jha et al. (2009)
Rain Shadow Rivers										
Los Reartes, Argentina	53	168	66	238	23	23	20	592	279	Lecomte et al. (2005)
Hawkesbury-Nepean, Australia	–	133	231	1074	46	1154	95	300	–	Markich and Brown (1998)

order: $HCO_3^- > Cl^- > SO_4^{2-}$ during all the seasons. Even though the Gibb's plot and mixing diagrams emphasize the significance of rock weathering and mineral dissolution as major hydrochemical drivers, the downstream trend of hydrochemistry parallel to the saturation trend in the Gibbs model and the scatter plot between Mg^{2+}/Na^+ and Mg^{2+}/Ca^{2+} imply the importance of evaporation in the downstream hydrochemistry. $Ca^{2+} + Mg^{2+}/Na^+ + K^+$, $Si/Na^+ + K^+$ as well as HCO_3^-/Ca^{2+} ratios suggest sources other than silicate weathering in PRB, e.g., atmospheric supply, dissolution of carbonate minerals and evaporitic deposits, anthropogenic inputs (domestic and farm/plantation residues). Relatively lower K^+/Na^+ ratios in the downstream imply less intense weathering, while higher ratios in the upstream might be derived from both weathering as well as anthropogenic inputs (i.e., fertilizer residues). The upstream segment shows considerably higher Cl^-/Na^+ ratios compared to downstream, which also indicate the hydrochemical modifications by anthropogenic interferences in the upstream catchments.

In Piper diagram, the water types between the upstream and downstream segments of PRB also show significant differences in that downstream samples are more enriched in HCO_3 compared to upstream samples, suggesting a spatial discrimination (in PRB) between upstream waters with anthropogenic modifications and downstream waters of groundwater-dominating discharge. Downstream waters of the basin have relatively higher $pCO_{2\ (river)}/pCO_{2\ (atmosphere)}$ during MON and PRM compared to upstream

samples, which also imply the significance of groundwater contributions toward the stream discharge. Even though the dissolved load in PRB is derived from various sources and processes, the contrasting hydrochemical behavior between upstream and downstream areas follows a marked geo-spatial trend, which is line with the rainfall gradient. Although spatial variability of rainfall in PRB shows a linear downstream (decreasing) trend, the best-fit model for the dissolved load suggests that the downstream hydrochemical variability in PRB (i.e., an increasing trend) is strongly non-linear and follows a power function ($f(x) = ax^k$).

Hence, as the proposed hypothesis, climate has a significant role in the spatial as well as temporal variations in hydrochemistry of PRB, which is calling for periodic monitoring of hydrochemistry of mountain river basins of rain shadow regions.

Acknowledgements

First author (JT) is indebted to (late) Dr. R. Satheesh (SES, Mahatma Gandhi University, Kerala) for moral support and mentoring during the early stages of research career. JT also acknowledges the helps rendered during chemical analyses by Ms. Manjusree, T.M. (Department of Environmental Sciences), the HOD (Department of Geology), University of Kerala and the Director, Central Ground Water Board, Thiruvananthapuram. Financial support from Kerala State Council for Science, Technology, and Environment, Thiruvananthapuram and permission and logistics for the field studies in the protected areas by Kerala Forest Department are also delightedly acknowledged. We are also grateful to the anonymous reviewers and the guest editor for their critical and helpful comments, which significantly improved the quality of the manuscript.

References

Ahearn, D.S., Sheibley, R.W., Dahlgren, R.A., Keller, K.E., 2004. Temporal dynamics of stream water chemistry in the last free-flowing river draining the western Sierra Nevada, California. J. Hydrol. 295 (1–4), 47–63. http://dx.doi.org/10.1016/j.jhydrol.2004.02.016.

Allan, J.D., 1995. Stream Ecology: Structure and Function of Running Waters. Chapman & Hall, London.

Anshumali, Ramanathan, A.L., 2007. Seasonal variation in the major ion chemistry of Pandoh Lake, Mandi District, Himachal Pradesh, India. Appl. Geochem. 22 (8), 1736–1747. http://dx.doi.org/10.1016/j.apgeochem.2007.03.045.

Banks, E.W., Simmons, C.T., Love, A.J., Shand, P., 2011. Assessing spatial and temporal connectivity between surface water and groundwater in a regional catchment: implications for regional scale water quantity and quality. J. Hydrol. 404 (1–2), 30–49. http://dx.doi.org/10.1016/j.jhydrol.2011.04.017.

Berner, E.K., Berner, R.A., 1987. The Global Water Cycle: Geochemistry and Environment. Prentice-Hall, New Jersey.

Berner, R.A., Berner, E.K., 1997. Silicate weathering and climate. In: Ruddiman, W.F. (Ed.), Tectonic Uplift and Climate Change. Plenum Press, New York, pp. 353–365.

Boulton, A.J., Findlay, S., Marmonier, P., Stanley, E.H., Valett, H.M., 1998. The functional significance of the hyporheic zone in streams and rivers. Annu. Rev. Ecol. Syst. 29, 59–81. http://dx.doi.org/10.1146/annurev.ecolsys.29.1.59.

Boulton, A.J., Marmonier, P., Davis, J.A., 1999. Hydrological exchange and subsurface water chemistry in streams varying in salinity in south-western Australia. Int. J. Salt Lake Res. 8 (4), 361–382. http://dx.doi.org/10.1007/BF02442121.

Brodie, J.E., Mitchell, A.W., 2005. Nutrients in Australian tropical rivers: changes with agricultural development and implications for receiving environments. Mar. Freshw. Res. 56 (3), 279–302. http://dx.doi.org/10.1071/MF04081.

Bucker, A., Crespo, P., Frede, H.-G., Vache, K., Cisneros, F., Breuer, L., 2010. Identifying controls on water chemistry of tropical cloud forest catchments: combining descriptive approaches and multivariate analysis. Aquat. Geochem. 16 (1), 127–149. http://dx.doi.org/10.1007/s10498-009-9073-4.

Buell, G.R., Peters, N.E., 1988. Atmospheric deposition effects on the chemistry of a stream in Northeastern Georgia. Water Air Soil Pollut. 39 (3–4), 275–291. http://dx.doi.org/10.1007/BF00279474.

Carpenter, S.R., Caraco, N.F., Correll, D.L., Howarth, R.W., Sharpley, A.N., Smith, V.H., 1998. Nonpoint pollution of surface waters with phosphorous and nitrogen. Ecol. Appl. 8 (3), 559–568. http://dx.doi.org/10.1890/1051-0761(1998)008[0559:NPOSWW]2.0.CO;2.

Chandrashekara, U.M., Sibichan, V., 2006. Logs and snags in a shola forest of Kerala, India. J. Mt. Sci. 3 (2), 131–138. http://dx.doi.org/10.1007/s11629-006-0131-8.

Chen, J., Wang, F., Xia, X., Zhang, L., 2002. Major element chemistry of the Changjiang (Yangtze River). Chem. Geol. 187 (3–4), 231–255. http://dx.doi.org/10.1016/S0009-2541(02)00032-3.

Crosa, G., Froebrich, J., Nikolayenko, V., Stefani, F., Galli, P., Calamari, D., 2006. Spatial and seasonal variations in the water quality of the Amu Darya River (Central Asia). Water Res. 40 (11), 2237–2245. http://dx.doi.org/10.1016/j.watres.2006.04.004.

Dalai, T.K., Krishnaswami, S., Sarin, M.M., 2002. Major ion chemistry in the headwaters of the Yamuna river system: chemical weathering, its temperature dependence and CO_2 consumption in the Himalaya. Geochim. Cosmochim. Acta 66 (19), 3397–3416. http://dx.doi.org/10.1016/S0016-7037(02)00937-7.

Das, A., Krishnaswami, S., 2006. Barium in Deccan Basalt rivers: its abundance, relative mobility and flux. Aquat. Geochem. 12 (3), 221–238. http://dx.doi.org/10.1007/s10498-005-5856-4.

Das, A., Krishnaswami, S., Sarin, M.M., Pande, K., 2005. Chemical weathering in the Krishna basin and Western Ghats of the Deccan Traps, India: rates of basalt weathering and their controls. Geochim. Cosmochim. Acta 69 (8), 2067–2084. http://dx.doi.org/10.1016/j.gca.2004.10.014.

Davies, B.R., Thoms, M.C., Walker, K.F., O'Keeffe, J.H., Gore, J.A., 1994. Dryland rivers: their ecology conservation and management. In: Calow, P., Petts, G.E. (Eds.), The Rivers Handbook: Hydrological and Ecological Principles. Blackwell, Oxford, UK. http://dx.doi.org/10.1002/9781444313871 (Chapter 25).

Drever, J.I., 1988. The Geochemistry of Natural Waters, second ed. Prentice-Hall, New York.

Eaton, A.D., Clesceri, L.S., Rice, E.W., Greenberg, A.E., Franson, M.A.H., 2005. Standard Methods for the Examination of Water and Wastewater, 21st ed. American Public Health Association (APHA), the American Water Works Association (AWWA), and the Water Environment Federation (WEF).

Edmond, J.M., Palmer, M.R., Measures, C.I., Brown, E.T., Huh, Y., 1996. Fluvial geochemistry of the eastern slope of the northeastern Andes and its foredeep in the drainage of the Orinoco in Colombia and Venezuela. Geochim. Cosmochim. Acta 60 (16), 2949–2974. http://dx.doi.org/10.1016/0016-7037(96)00142-1.

Frazee Jr., J.M., 1982. Geochemical pattern analysis-method of describing the southeastern limestone regional aquifer system. In: Beck, B.F. (Ed.), Studies of the Hydrogeology of the Southeastern United States. Georgia Southwestern College, Americus, Special Publications No. 1, pp. 46–58.

Frohlich, H.L., Breuer, L., Frede, H.-G., Huisman, J.A., Vache, K.B., 2008. Water source characterization through spatiotemporal patterns of major, minor and trace element stream concentrations in a complex, mesoscale German catchment. Hydrol. Process. 22 (12), 2028–2043. http://dx.doi.org/10.1002/hyp.6804.

Gaillardet, J., Dupre, B., Louvat, P., Allegre, C.J., 1999. Global silicate weathering and CO_2 consumption rates deduced from the chemistry of large rivers. Chem. Geol. 159 (1–4), 3–30. http://dx.doi.org/10.1016/S0009-2541(99)00031-5.

Galy, A., France-Lanord, C., 1999. Weathering processes in the Ganges–Brahmaputra basin and the riverine alkalinity budget. Chem. Geol. 159 (1–4), 31–60. http://dx.doi.org/10.1016/S0009-2541(99)00033-9.

Gibbs, R.J., 1970. Mechanisms controlling world water chemistry. Science 170 (3962), 1088–1090. http://dx.doi.org/10.1126/science.170.3962.1088.

GSI, 1992. District Resource Map, Idukki District, Kerala. Part-I. Geology and Minerals. Geological Survey of India, Kolkata.

GSI, 2005. Geological and Mineral Map of Kerala. Miscellaneous Publication No. 30 (IX) Geological Survey of India, Hyderabad.

Gupta, H., Chakrapani, G.J., Selvaraj, K., Kao, S.-J., 2011. The fluvial geochemistry, contributions of silicate, carbonate and saline–alkaline components to chemical weathering flux and controlling parameters: Narmada River (Deccan Traps), India. Geochim. Cosmochim. Acta 75 (3), 800–824. http://dx.doi.org/10.1016/j.gca.2010.11.010.

Gurumurthy, G.P., Balakrishna, K., Riotte, J., Braun, J.-J., Audry, S., Udaya Shankar, H.N., Manjunatha, B.R., 2012. Controls on intense silicate weathering in a tropical river, southwestern India. Chem. Geol. 61–69. http://dx.doi.org/10.1016/j.chemgeo.2012.01.016.

Harmon, R.S., Lyons, W.B., Long, D.T., Ogden, F.L., Mitasova, H., Gardner, C.B., Welch, K.A., Witherow, R.A., 2009. Geochemistry of four tropical montane watersheds, Central Panama. Appl. Geochem. 24 (4), 624–640. http://dx.doi.org/10.1016/j.apgeochem.2008.12.014.

Hem, J.D., 1948. Fluctuations in concentration of dissolved solids of some southwestern streams. Trans. Am. Geophys. Union 29 (1), 80–84.

Hu, M.-H., Stallard, R.F., Edmond, J.M., 1982. Major ion chemistry of some large Chinese rivers. Nature 298, 550–553. http://dx.doi.org/10.1038/298550a0.

Jennerjahn, T.C., Ittekkot, V., Klopper, S., Adi, S., Purwo Nugroho, S., Sudiana, N., Yusmal, A., Prihartanto, Gaye-Haake, B., 2004. Biogeochemistry of a tropical river affected by human activities in its catchment: Brantas River estuary and coastal waters of Madura Strait, Java, Indonesia. Estuar. Coast. Shelf Sci. 60 (3), 503–514. http://dx.doi.org/10.1016/j.ecss.2004.02.008.

Jennerjahn, T.C., Soman, K., Ittekkot, V., Nordhaus, I., Sooraj, S., Priya, R.S., Lahajnar, N., 2008. Effect of land use on the biogeochemistry of dissolved nutrients and suspended and sedimentary organic matter in the tropical Kallada River and Ashtamudi estuary, Kerala, India. Biogeochemistry 90 (1), 29–47. http://dx.doi.org/10.1007/s10533-008-9228-1.

Jha, P.K., Tiwari, J., Singh, U.K., Kumar, M., Subramanian, V., 2009. Chemical weathering and associated CO2 consumption in the Godavari river basin, India. Chem. Geol. 264 (1–4), 364–374. http://dx.doi.org/10.1016/j.chemgeo.2009.03.025.

Jose, S., Sreepathy, A., Kumar, B.M., Venugopal, V.K., 1994. Structural, floristic and edaphic attributes of the grassland-shola forests of Eravikulam in peninsular

India. For. Ecol. Manage. 65 (2–3), 279–291. http://dx.doi.org/10.1016/0378-1127(94)90176-7.
Lecomte, K.L., Pasquini, A.I., Depetris, P.J., 2005. Mineral weathering in a semiarid mountain river: its assessment through PHREEQC inverse modeling. Aquat. Geochem. 11 (2), 173–194. http://dx.doi.org/10.1007/s10498-004-3523-9.
Leite, M.G.P., Fujaco, M.A.G., Nalini Jr., H.A., Castro, P.T.A., 2010. Influence of geology in the geochemistry signature of Itacolomi State Park waters, Minas Gerais-Brazil. Environ. Earth Sci. 60 (8), 1723–1730. http://dx.doi.org/10.1007/s12665-009-0306-z.
Lesack, L.F.W., Hecky, R.E., Melack, J.M., 1984. Transport of carbon, nitrogen, phosphorus, and major solutes in the Gambia River, West Africa. Limnol. Oceanogr. 29 (4), 816–830. http://dx.doi.org/10.4319/lo.1984.29.4.0816.
Lewis Jr., W.M., Hamilton, S.K., Jones, S.L., Runnels, D.D., 1987. Major element chemistry, weathering and element yields for the Caura River drainage, Venezuela. Biogeochemistry 4 (2), 159–181. http://dx.doi.org/10.1007/BF02180153.
Li, S., Zhang, Q., 2008. Geochemistry of the upper Han River basin, China, 1: spatial distribution of major ion compositions and their controlling factors. Appl. Geochem. 23 (12), 3535–3544. http://dx.doi.org/10.1016/j.apgeochem.2008.08.012.
Lloret, E., Dessert, C., Gaillardet, J., Alberic, P., Crispi, O., Chaduteau, C., Benedetti, M.F., 2011. Comparison of dissolved inorganic and organic carbon yields and fluxes in the watersheds of tropical volcanic islands, examples from Guadeloupe (French West Indies). Chem. Geol. 280 (1–2), 65–78. http://dx.doi.org/10.1016/j.chemgeo.2010.10.016.
Lloret, E., Dessert, C., Pastor, L., Lajeunesse, E., Crispi, O., Gaillardet, J., Benedetti, M.F., 2013. Dynamic of particulate and dissolved organic carbon in small volcanic mountainous tropical watersheds. Chem. Geol. 351, 229–244. http://dx.doi.org/10.1016/j.chemgeo.2013.05.023.
Magaritz, M., Aravena, R., Pena, H., Suzuki, O., Grilli, A., 1989. Water chemistry and isotope study of streams and springs in northern Chile. J. Hydrol. 108, 323–341. http://dx.doi.org/10.1016/0022-1694(89)90292-8.
Markich, S.J., Brown, P.L., 1998. Relative importance of natural and anthropogenic influences on the fresh surface water chemistry of the Hawkesbury–Nepean River, south-eastern Australia. Sci. Total Environ. 217 (3), 201–230. http://dx.doi.org/10.1016/S0048-9697(98)00188-0.
Maya, K., Babu, K.N., Padmalal, D., Seralathan, P., 2007. Hydrochemistry and dissolved nutrient flux of two small catchment rivers, south-western India. Chem. Ecol. 23 (1), 13–27. http://dx.doi.org/10.1080/02757540601084029.
McDowell, W.H., Asbury, C.E., 1994. Export of carbon, nitrogen, and major ions from three tropical montane watersheds. Limnol. Oceanogr. 39 (1), 111–125. http://dx.doi.org/10.4319/lo.1994.39.1.0111.
McDowell, W.H., Lugo, A.E., James, A., 1995. Export of nutrients and major ions from Caribbean catchments. J. North Am. Benthol. Soc. 14 (1), 12–20.
Meybeck, M., 1987. Global chemical weathering of surficial rocks estimated from river dissolved loads. Am. J. Sci. 287 (5), 401–428. http://dx.doi.org/10.2475/ajs.287.5.401.
Meyer, J.L., McDowell, W.H., Bott, T.L., Elwood, J.W., Ishizaki, C., Melack, J.M., Peckarsky, B.L., Peterson, B.J., Rublee, P.A., 1988. Elemental dynamics in streams. J. North Am. Benthol. Soc. 7 (4), 410–432.
Milliman, J.D., Meade, R.H., 1983. World-wide delivery of river sediment to the oceans. J. Geol. 91 (1), 1–21.
Milliman, J.D., Syvitski, J.P.M., 1992. Geomorphic/tectonic control of sediment discharge to the ocean: the importance of small mountainous rivers. J. Geol. 100 (5), 525–544.
Millot, R., Gaillardet, J., Dupre, B., Allegre, C.J., 2002. The global control of silicate weathering rates and the coupling with physical erosion: new insights from rivers of the Canadian Shield. Earth Planet. Sci. Lett. 196 (1–2), 83–98. http://dx.doi.org/10.1016/S0012-821X(01)00599-4.
Mortatti, J., Probst, J.-L., 2003. Silicate rock weathering and atmospheric/soil CO_2 uptake in the Amazon basin estimated from river water geochemistry: seasonal and spatial variations. Chem. Geol. 197 (1–4), 177–196. http://dx.doi.org/10.1016/S0009-2541(02)00349-2.
Moyer, R.P., Bauer, J.E., Grottoli, A.G., 2013. Carbon isotope biogeochemistry of tropical small mountainous river, estuarine, and coastal systems of Puerto Rico. Biogeochemistry 112 (1–3), 589–612. http://dx.doi.org/10.1007/s10533-012-9751-y.
Murphy, S.F., Stallard, R.F. (Eds.), 2012. Water Quality and Landscape Processes of Four Watersheds in Eastern Puerto Rico. U.S. Geological Survey Professional Paper 1789, 292 p.
Ovalle, A.R.C., Silva, C.F., Rezende, C.E., Gatts, C.E.N., Suzuki, M.S., Figueiredo, R.O., 2013. Long-term trends in hydrochemistry in the Paraiba do Sul River, south-eastern Brazil. J. Hydrol. 481, 191–203. http://dx.doi.org/10.1016/j.jhydrol.2012.12.036.
Peters, N.E., Ratcliffe, E.B., 1998. Tracing hydrologic pathways using chloride at the Panola Mountain research watershed, Georgia, USA. Water Air Soil Pollut. 105 (1–2), 263–275. http://dx.doi.org/10.1023/A:1005082332332.
Piper, A.M., 1944. A graphic procedure in the geochemical interpretation of water-analyses. Trans. Am. Geophys. Union 25 (6), 914–928.
Pradhan, U.K., Wu, Y., Shirodkar, P.V., Zhang, J., 2014. Seasonal nutrient chemistry in mountainous river systems of tropical Western Peninsular India. Chem. Ecol. http://dx.doi.org/10.1080/02757540.2014.961438.
Prasad, M.B.K., Ramanathan, A.L., 2005. Solute sources and processes in the Achankovil river basin, Western Ghats, southern India. Hydrol. Sci. J. 50 (2), 341–354. http://dx.doi.org/10.1623/hysj.50.2.341.61798.
Probst, J.-L., Nkounkou, R.-R., Krempp, G., Bricquet, J.-P., Thiebaux, J.-P., Olivry, J.-C., 1992. Dissolved major elements exported by the Congo and the Ubangi rivers during the period 1987–1989. J. Hydrol. 135 (1–4), 237–257. http://dx.doi.org/10.1016/0022-1694(92)90090-I.
Psenner, R., Schmidt, R., 1992. Climate-driven pH control of remote alpine lakes and effects of acid deposition. Nature 356, 781–783. http://dx.doi.org/10.1038/356781a0.
Radhakrishna, B.P., Vaidyanadhan, R., 1997. Geology of Karnataka, second ed. Geological Society of India, Bangalore.
Raymahashay, B.C., 1986. Geochemistry of bicarbonate in river water. J. Geol. Soc. India 27 (1), 114–118.
Sarin, M.M., Krishnaswami, S., Trivedi, J.R., Sharma, K.K., 1992. Major ion chemistry of the Ganga source waters: weathering in the high altitude Himalaya. Proc. Ind. Acad. Sci. Earth Planet. Sci. 101 (1), 89–98.
Schultz, A.M., Begemann, M.H., Schmidt, D.A., Weathers, K.C., 1993. Longitudinal trends in pH and aluminium chemistry of the Coxing Kill, Ulster County, New York. Water Air Soil Pollut. 69 (1–2), 113–125. http://dx.doi.org/10.1007/BF00478352.
Singh, K.P., Malik, A., Mohan, D., Sinha, S., 2004. Multivariate statistical techniques for the evaluation of spatial and temporal variations in water quality of Gomti River (India): a case study. Water Res. 38 (18), 3980–3992. http://dx.doi.org/10.1016/j.watres.2004.06.011.
Smolders, A.J.P., Hudson-Edwards, K.A., Van der Velde, G., Roelofs, J.G.M., 2004. Controls on water chemistry of the Pilcomayo river (Bolivia, South-America). Appl. Geochem. 19 (11), 1745–1758. http://dx.doi.org/10.1016/j.apgeochem.2004.05.001.
Soman, K., 2002. Geology of Kerala. Geological Society of India, Bangalore.
Sommaruga-Wograth, S., Koinig, K.A., Schmidt, R., Sommaruga, R., Tessadri, R., Psenner, R., 1997. Temperature effects on the acidity of remote alpine lakes. Nature 387, 64–67. http://dx.doi.org/10.1038/387064a0.
SSO, 2007. Benchmark Soils of Kerala. Soil Survey Organization. Department of Agriculture, Government of Kerala, Kerala, India.
Stallard, R.F., Edmond, J.M., 1981. Geochemistry of the Amazon: 1. Precipitation chemistry and the marine contribution to the dissolved load at the time of peak discharge. J. Geophys. Res. Oceans 86 (C10), 9844–9858. http://dx.doi.org/10.1029/JC086iC10p09844.
Stallard, R.F., Edmond, J.M., 1983. Geochemistry of the Amazon: 2. The influence of geology and weathering environment on the dissolved load. J. Geophys. Res. Oceans 88 (C14), 9671–9688.
Stallard, R.F., Edmond, J.M., 1987. Geochemistry of the Amazon: 3. Weathering chemistry and limits to dissolved inputs. J. Geophys. Res. Oceans 92 (C8), 8293–8302. http://dx.doi.org/10.1029/JC092iC08p08293.
Stallard, R.F., Koehnken, L., Johnsson, M.J., 1991. Weathering processes and the composition of inorganic material transported through the Orinoco River system, Venezuela and Colombia. Geoderma 51 (1–4), 133–165. http://dx.doi.org/10.1016/0016-7061(91)90069-6.
Stumm, W., Morgan, J.J., 1996. Aquatic Chemistry: Chemical Equilibria and Rates in Natural Waters. John Wiley & Sons, New York.
Stutter, M.I., Deeks, L.K., Low, D., Billett, M.F., 2006. Impact of soil and groundwater heterogeneity on surface water chemistry in an upland catchment. J. Hydrol. 318 (1–4), 103–120. http://dx.doi.org/10.1016/j.jhydrol.2005.06.007.
Subramanian, V., 1983. Factors controlling the chemical composition of river waters of India. Proc. Int. Assoc. Hydrol. Sci. Symp. Hamburg 141, 145–151.
Thomas, J., 2012. Channel Characteristics of Two Upland River Basins of Contrasting Climate: A Study from Kerala. Ph.D. Dissertation. University of Kerala, Thiruvananthapuram, Kerala, India.
Thomas, J., Joseph, S., Thrivikramji, K.P., Abe, G., 2011. Morphometric analysis of the drainage system and its hydrological implications in the rain shadow regions, Kerala, India. J. Geog. Sci. 21 (6), 1077–1088. http://dx.doi.org/10.1007/s11442-011-0901-2.
Thomas, J., Joseph, S., Thrivikramji, K.P., Abe, G., Kannan, N., 2012. Morphometrical analysis of two tropical mountain river basins of contrasting environmental settings, the southern Western Ghats, India. Environ. Earth Sci. 66 (8), 2353–2366. http://dx.doi.org/10.1007/s12665-011-1457-2.
Thomas, J., Joseph, S., Thrivikramji, K.P., Manjusree, T.M., Arunkumar, K.S., 2014. Seasonal variation in major ion chemistry of a tropical mountain river, the southern Western Ghats, Kerala, India. Environ. Earth Sci. 71 (5), 2333–2351. http://dx.doi.org/10.1007/s12665-013-2634-2.
Thomas, J., Joseph, S., Thrivikramji, K.P., 2015. Hydrogeochemical drivers and processes controlling solute chemistry of two mountain river basins of contrasting climates in the southern Western Ghats, India. In: Ramkumar, Mu, Kumaraswamy, K., Mohanraj, R. (Eds.), Environmental Management of River Basin Ecosystems. Springer-Verlag, Heidelberg, pp. 355–396. http://dx.doi.org/10.1007/978-3-319-13425-3_17.
Townsend, C.R., Hildrew, A.G., Francis, J., 1983. Community structure in some southern English streams: the influence of physicochemical factors. Freshw. Biol. 13 (6), 521–544. http://dx.doi.org/10.1111/j.1365-2427.1983.tb00011.x.
Townsend-Small, A., McClain, M.E., Hall, B., Noguera, J.L., Llerena, C.A., Brandes, J.A., 2008. Suspended sediments and organic matter in mountain headwaters of the Amazon River: results from a 1-year time series study in the central Peruvian Andes. Geochim. Cosmochim. Acta 72 (3), 732–740. http://dx.doi.org/10.1016/j.gca.2007.11.020.
Upchurch, S.B., 1992. Quality of water in Florida's aquifer systems. In: Maddox, G.L., Lloyd, J.M., Scott, T.M., Upchurch, S.B., Copeland, R. (Eds.), Florida's Groundwater Quality Monitoring Programme: Background Hydrochemistry. Florida

Geological Society, Tallahassee, Special Publication No. 34, pp. 12–51.
Vegas-Vilarrubia, T., Maass, M., Rull, V., Elias, V., Ovalle, A.R.C., Lopez, D., Schneider, G., Depetris, P.J., Douglas, I., 1994. Small catchment studies in the tropical zone. In: Moldan, B., Cerny, J. (Eds.), Biogeochemistry of Small Catchments: A Tool for Environmental Research. SCOPE 51. John Wiley & Sons, New York, pp. 343–360.
Wheater, H.S., Kleissen, F.M., Beck, M.B., Tuck, S., Jenkins, A., Harriman, R., 1990. Modeling short-term flow and chemical response in the Allt a' Mharcaidh catchment. In: Mason, B.J. (Ed.), The Surface Waters Acidification Programme. Cambridge University Press, Cambridge, pp. 477–483.
White, A.F., Blum, A.E., 1995. Effects of climate on chemical weathering in watersheds. Geochim. Cosmochim. Acta 59 (9), 1729–1747. http://dx.doi.org/10.1016/0016-7037(95)00078-E.
WHO, 2011. Guidelines for Drinking-Water Quality, fourth ed. World Health Organization, WHO Press, Geneva.
Wohl, E., Barros, A., Brunsell, N., Chappell, N.A., Coe, M., Giambelluca, T., Goldsmith, S., Harmon, R., Hendrickx, J.M.H., Juvik, J., McDonnell, J., Ogden, F., 2012. The hydrology of the humid tropics. Nat. Clim. Change 2 (9), 655–662. http://dx.doi.org/10.1038/nclimate1556.
Zhu, B., Yang, X., Rioual, P., Qin, X., Liu, Z., Xiong, H., Yu, J., 2011. Hydrogeochemistry of three watersheds (the Erlqis, Zhungarer and Yili) in northern Xinjiang, NW China. Appl. Geochem. 26 (8), 1535–1548. http://dx.doi.org/10.1016/j.apgeochem.2011.06.018.